UNIVERSITEIT•STELLENBOSCH•UNIVERSITY
jou kennisvennoot • your knowledge partner

Design of an Electrical Power System for a PocketQube

Dean Jeggels
23676787

Report submitted in partial fulfilment of the requirements of the module Project (E) 448 for the degree Baccalaureus in Engineering in the Department of Electrical and Electronic Engineering at Stellenbosch University.

Supervisor: Dr A. Barnard

November 2023

Acknowledgements

I extend my deepest gratitude to my parents, Mom and Dad, and my Brother for their unwavering support, continuous motivation, and heartfelt prayers throughout my life. Their encouragement has been my driving force.

In loving memory of my late Uncle Steven, whose inspiration led me to pursue a path in electrical and electronic engineering. His legacy lives on in my journey.

A special thanks to my friends and extended family for standing by my side through thick and thin, always providing a source of unmatched banter and camaraderie.

I express my sincere appreciation to Dr. Barnard for his invaluable guidance and unwavering support as my project supervisor. His mentorship has been instrumental in shaping the trajectory of my work.

Acknowledgment is also due to Mev. Wendy Kannemeyer, whose skilled hands expertly handled the delicate task of soldering microelectronic components. I am grateful to Mev Jenny Martin and Ms. Candice Daniels for their pivotal roles in procurement tasks, including the seamless ordering of essential components.

To all those mentioned and the countless others who have contributed to my journey, I extend my heartfelt thanks. Your support has been instrumental in making this project a reality.

UNIVERSITEIT·STELLENBOSCH·UNIVERSITY
jou kennisvennoot • your knowledge partner

Plagiaatverklaring / *Plagiarism Declaration*

1. Plagiaat is die oorneem en gebruik van die idees, materiaal en ander intellektuele eiendom van ander persone asof dit jou eie werk is.
   Plagiarism is the use of ideas, material and other intellectual property of another's work and to present is as my own.

2. Ek erken dat die pleeg van plagiaat 'n strafbare oortreding is aangesien dit 'n vorm van diefstal is.
   I agree that plagiarism is a punishable offence because it constitutes theft.

3. Ek verstaan ook dat direkte vertalings plagiaat is.
   I also understand that direct translations are plagiarism.

4. Dienooreenkomstig is alle aanhalings en bydraes vanuit enige bron (ingesluit die internet) volledig verwys (erken). Ek erken dat die woordelikse aanhaal van teks sonder aanhalingstekens (selfs al word die bron volledig erken) plagiaat is.
   Accordingly all quotations and contributions from any source whatsoever (including the internet) have been cited fully. I understand that the reproduction of text without quotation marks (even when the source is cited) is plagiarism

5. Ek verklaar dat die werk in hierdie skryfstuk vervat, behalwe waar anders aangedui, my eie oorspronklike werk is en dat ek dit nie vantevore in die geheel of gedeeltelik ingehandig het vir bepunting in hierdie module/werkstuk of 'n ander module/werkstuk nie.
   I declare that the work contained in this assignment, except where otherwise stated, is my original work and that I have not previously (in its entirety or in part) submitted it for grading in this module/assignment or another module/assignment.

23676787 Studentenommer / *Student number*	Deggels Handtekening / *Signature*
DE. Jeggels Voorletters en van / *Initials and surname*	November 5, 2023 Datum / *Date*

Abstract

English

This project focuses on the design and implementation of an Electrical Power System (EPS) tailored for a PocketQube picosatellite, employing Maximum Power Point Tracking (MPPT) technology for solar energy harvesting. The EPS efficiently stores solar energy in batteries, serving as a crucial lifeline to power the satellite's bus system and various subsystems. Telemetry readings play a vital role in overseeing EPS parameters, emphasizing the project's goal of delivering an efficient, lightweight system aligned with PocketQube standards. It addresses key questions regarding energy needs, harvesting efficiency and the integration of components within the PQ9 physical constraints 1P form factor. The outlined methodology includes a literature review, system design, prototyping, testing and integration into the PocketQube platform, contributing to advancements in picosatellite technology and offering valuable insights for future EPS implementations on PocketQubes.

Afrikaans

Hierdie projek fokus op die ontwerp en implementering van 'n Elektriese Kragstelsel (EPS) geskep vir 'n PocketQube pikosatelliet, waar gebruik gemaak word van Maksimum Kragpunt Volg (MPPT) tegnologie vir sonenergie-oes. Die EPS stoor sonenergie effektief in batterye, wat as 'n noodsaaklike lewenslyn dien vir die satelliet se busstelsel en verskeie subsisteme. Telemetrie-lesings speel 'n noodsaaklike rol in die toesig oor EPS-parameter, en beklemtoon die projek se doelwit om 'n effektiewe, ligte sisteem te lewer wat voldoen aan die standaarde van die PocketQube. Dit spreek sleutelvrae aan rakende energiebehoeftes, oesdoeltreffendheid, en die integrasie van komponente binne die PQ9 fisiese beperkings van 'n 1P vormfaktor. Die uitgeligte metodologie sluit 'n literatuurstudie, stelselontwerp, prototipering, toetsing, en integrasie in die PocketQube platform in, wat bydra tot vooruitgang in pikosatelliet tegnologie en waardevolle insigte bied vir toekomstige EPS-implementasies op PocketQubes.

Contents

Declaration ii

Abstract iii

List of Figures vii

List of Tables ix

Nomenclature x

Chapter 1: Introduction 1

1.1. Background and motivation 1
1.2. Research Questions and Goals 2
1.3. Outline 3

Chapter 2: Literature Review 4

2.1. PocketQube Standard 4
2.2. PocketQube Electrical Power System 5
2.2.1. Photovoltaic cells 6
2.2.2. Solar Cell characteristics 7
2.3. Power Regulating 8
2.3.1. Buck Converter 8
2.3.2. Boost Converter 10
2.4. Maximum Power Point Tracking techniques 12
2.4.1. Perturb & Observe Algorithm 12
2.4.2. Incremental Conductance Algorithm 13
2.4.3. Constant Voltage Algorithm 14
2.5. Battery Management Systems 15
2.5.1. Lithium Ion Batteries 15
2.5.2. Battery charging methods 17

Chapter 3: Detail Design 19

3.1. System Diagram 19
3.2. MPPT 20
3.2.1. Hardware 20

3.2.2. Software . . . 21
3.2.3. MPPT Experimental Design . . . 23
3.3. Battery Management System . . . 24
3.3.1. Battery Charging . . . 24
3.3.2. Battery protection . . . 25
3.3.3. BMS Experimental Design . . . 27
3.4. Voltage Regulation . . . 29
3.4.1. Regulated 3.3V . . . 29
3.4.2. Regulated 5V . . . 29
3.4.3. Regulators Experimental Design . . . 30
3.5. Overcurrent Protection . . . 30
3.5.1. Switches . . . 30
3.5.2. Current sensing . . . 31
3.5.3. Overcurrent Protection Experimental Design . . . 32
3.6. PCB Design . . . 32

Chapter 4: Experiments and Results **34**
4.1. Regulators . . . 34
4.2. Overcurrent Protection . . . 36
4.3. MPPT . . . 36
4.4. BMS . . . 38

Chapter 5: Conclusion **41**
5.1. MPPT System . . . 41
5.2. Battery Management System (BMS) . . . 41
5.3. Regulators . . . 41
5.4. Challenges and Recommendations . . . 42

Bibliography **43**

A. Project Planning Schedule **46**

B. Outcomes Compliance **47**

C. Components Characteristics **50**
C.1. LTC3130-1 . . . 50
C.2. ATmega328P . . . 51
C.3. MP3414A . . . 52
C.4. LTC4066 . . . 53
C.5. Li-ion Battery . . . 54
C.6. BQ29700 . . . 55

D. Results Graphs and Tables **57**

E. Schematics **65**

F. Code **81**

List of Figures

1.1. The PocketQube satellite. 2
2.1. PocketQube Mechanical Interface. 4
2.2. Self-derived representation of PocketQube Subsystems designed by each student within the group. 5
2.3. The EPS subsystem. 6
2.4. Photo-generated voltage and current 7
2.6. a Simple resistive divider 8
2.7. Buck Converter 9
2.8. Boost Converter 11
2.9. Four trends in a P-V graph for a PV cell 12
2.10. The P&O algorithm. 13
2.11. Incremental Conductance 14
2.12. Energy Densities of different battery types 16
2.13. Electrochemical composition of a li-ion battery 16
2.14. CCCV algorithm 18
3.1. Proposed EPS subsystem 19
3.2. LTC3130-1: Typical Application. 20
3.3. MPPC amplifier with external resistor divider 21
3.4. LTC4066: Typical Application and Simplified Block Diagram. 24
3.5. BQ29700: Typical Application. 26
3.6. Typical Application for MP3414. 29
3.7. TPS2561: Typical Application. 30
3.8. INA138: Typical Application. 31
3.9. Integrated Current sensor circuit 32
3.10. PCB Prototype 1 33
4.1. LTC3130-1: Typical Characteristics. 34
4.2. MP3414: Typical Characteristics. 35
4.3. Typical I-V and P-V characteristics of a PV Cell 36
4.4. MPPT panel power after 30 min 37
4.5. Charge Current vs. Charge Voltage expectation. 38
4.6. Combined Charge Current vs. Charge Voltage based on different charging methods. 39

A.1. Project Gantt Chart 46

C.1. Functional Block Diagram for BQ29700. 55
C.2. Test Circuits for BQ29700. 56

D.1. Charge Current vs. Charge Voltage based on Table D.4. 58
D.2. Charge Current vs. Charge Voltage based on Table D.5. 59
D.3. Charge Current vs. Charge Voltage based on Table D.6. 59
D.4. I-V Characteristics of Panels 62
D.5. P-V Characteristics of Panels 62

List of Tables

2.1. Dimensions of Units. 4
2.2. Backplane Pin Definitions. 5
3.1. V_{OUT} Program settings for LTC3130-1 21
4.1. $V_{IN} = 3.7V$ 35
4.2. Maximum Power Points for Different Tests 37
4.3. Test Results for BQ29700 Design Parameters 40

A.1. Project Schedule 46

C.1. Desired Characteristics of LTC3130-1 for MPPT. 50
C.2. Desired Characteristics of ATmega328P 8-bit AVR Microcontroller. 51
C.3. Desired Characteristics of MP3414A. 52
C.4. Desired Characteristics of LTC4066 for Battery Charging and Power Management. 53
C.5. Test Battery Specifications. 54
C.6. Ordered Battery Specifications. 54
C.7. Design Parameters for BQ29700. 55

D.1. $V_{IN} = 3V$ 57
D.2. $V_{IN} = 3.3V$ 57
D.3. $V_{IN} = 5V$ 57
D.4. Li-ion Battery Parameters During Charging on Bench Power Supply . . . 58
D.5. Li-ion Battery Parameters During Charging on PocketQube with USB . . . 60
D.6. Li-ion Battery Parameters During Charging on PocketQube with MPPT . 61
D.7. MPPT Algorithm Results and Accuracy at high load 63
D.8. MPPT Algorithm Results and Accuracy at low load 64

Nomenclature

Acronyms and abbreviations

MPPT	Maximum Power Point Tracking
MPP	Maximum Power Point
EPS	Electrical Power System
Li-ion	lithium-ion
P&O	Perturb and Observe
PV	Photovoltaic
IC	Incremental Conductance
BMS	Battery Management System
PWM	Pulse Width Modulation
UVLO	Undervoltage Lockout
NTC	Negative Temperature Coefficient
SOC	State of Charge
DOD	Depth of Discharge
CV	Constant Voltage
CC	Constant Current
CCCV	Constant Current Constant Voltage
PCB	Printed Circuit Board
ADCS	Attitude Determination and Control System
OBC	On Board Computer
COMM	Communications link
EN	Enable
CAD	Computer Aided Design
ADC	Analog-to-Digital Converter
GND	Ground

Chapter 1: Introduction

The primary objective of this project is to design and implement an Electrical Power System (EPS) tailored for a PocketQube picosatellite. This system harvests solar energy through the utilization of Maximum Power Point Tracking (MPPT) technology. The EPS will efficiently store solar energy in batteries, subsequently powering the satellite's bus system and various subsystems through either the solar cells or batteries serving as a crucial lifeline to the satellite.

Telemetry readings will play a crucial role in overseeing critical parameters of the EPS. The project's overarching goal is to deliver an efficient, lightweight and space-constrained EPS that aligns with the specifications of the PocketQube standard. This involves a comprehensive process, econtaining requirement analysis, solar cell selection, MPPT algorithm development, battery choice, a battery management system to ensure the protection of the batteries in the long term, charging and discharging of the batteries and the establishment of a power regulation and distribution network.

The proposed methodology includes conducting a literature review, system design, prototyping, and rigorous testing. The final stages will involve miniaturization and seamless integration into the PocketQube picosatellite platform.

1.1. Background and motivation

This individual project forms part of the final year thesis project for Electrical & Electronic Engineering students at the University of Stellenbosch. The project topic, Design of an Electrical Power System for a PocketQube, was proposed by Dr. Arno Barnard, who also served as the project supervisor. The PocketQube serves as an educational platform for students which exposes them to design challenges within the space environment as well as learning and testing engineering skills in the process.

The PocketQube concept in Figure 1.1 originated in 2009, proposed by Professor Robert J. Twiggs through collaboration between Morehead State University and Kentucky Space. Standards for the PocketQube were established to facilitate space applications for universities. PocketQubes are cube-shaped satellites measuring 50x50 mm, with a maximum mass of 250 g, commonly employing off the shelf components [1].

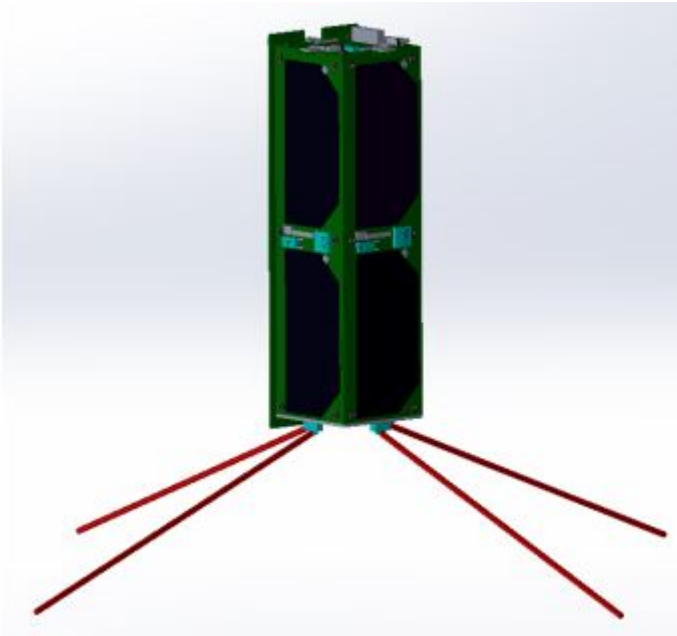

Figure 1.1: The PocketQube satellite. Reproduced from [1].

1.2. Research Questions and Goals

The goals of this project are derived from the following research questions:

- **Question 1:** How much energy is needed and available for the PocketQube?
  - **Goal 1:** Quantify the energy requirements of a PocketQube mission under various operational scenarios.
  - **Goal 2:** Assess the sources of available energy.
- **Question 2:** How can we harvest this energy as efficiently as possible?
  - **Goal 3:** Investigate and design efficient energy harvesting systems compatible with the PocketQube form factor.
  - **Goal 4:** Optimize the energy harvesting process to maximize power generation under varying mission conditions.
- **Question 3:** How should the energy be stored and distributed to other subsystems of the PocketQube?
  - **Goal 5:** Explore energy storage options suitable for the PocketQube, considering factors such as energy density, weight, and reliability.
  - **Goal 6:** Develop an efficient energy distribution system to supply power to different subsystems.

- **Question 4:**How can we implement all this onto a PCB with the PQ9 physical constraints 1P form factor?
  - **Goal 7:** Design a Printed Circuit Board (PCB) layout that accommodates energy harvesting, storage, and distribution components within the constraints of the PQ9 1P form factor.
  - **Goal 8:** Validate the feasibility of the PCB design through testing, ensuring compatibility with the PocketQube's physical and electrical requirements.

These goals collectively aim to address the research questions and contribute to the development of an efficient and viable energy management system for PocketQube satellites.

1.3. Outline

The outline of this project is to provide a walk through of the process to ultimately reach the goals above, similarly to the flow of power through the system. Starting from the harvesting of power from the sun, through the regulation of power to and from the batteries, before reaching the appropriate bus lines to the subsystems

In Chapter 2 the literature review is done. The PocketQube standard for this project is briefly discussed before diving into the working principle behind semiconductor devices, solar cells, that convert solar energy to electrical energy on the PocketQubes surface. The techniques for regulating this newly harvested energy as efficiently as possible is further described before then diving into the theory of batteries and how to charge and manage it for extended periods of time.

In Chapter 3, the theory discussed in the previous chapter is now utilized into the design of the hardware and software of the EPS before eventually designed onto a PCB.

Chapter 4 presents the testing and results that has been done on the various components of the system.

Chapter 5 concludes the thesis with what the test results mean and how it can be used in the future to either redesign or implement the EPS for a PocketQube.

Chapter 2: Literature Review

2.1. PocketQube Standard

The PocketQube standard is a specification for a type of picosatellite with the dimensions of a 50mm cube. This is know as a "1P", however scaled up versions known as "2P" and "3P" have been developed according to the dimensions in Table 2.1. It is also important to note that the PocketQube is deployed using a sliding backplate which causes one side of the platform to have slightly different dimensions as shown in Table 2.1

Table 2.1: Dimensions of Units. Reproduced from [1].

Number of Units (P)	External Dimensions without Backplate (mm)	Sliding Backplate Dimension (mm)
1P	50x50x50	58x64x1.6
2P	50x50x114	58x128x1.6
3P	50x50x178	58x192x1.6

For this project each module of the PocketQube follows the PQ9 and CS214 standard which defines the dimensions and backplane header connections, in Figure 2.1 and Table 2.2, to ensure consistency throughout the development of all modules within the PocketQube.

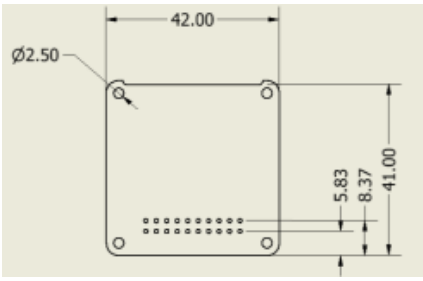

(a) PocketQube Module Dimensions. Reproduced from [2].

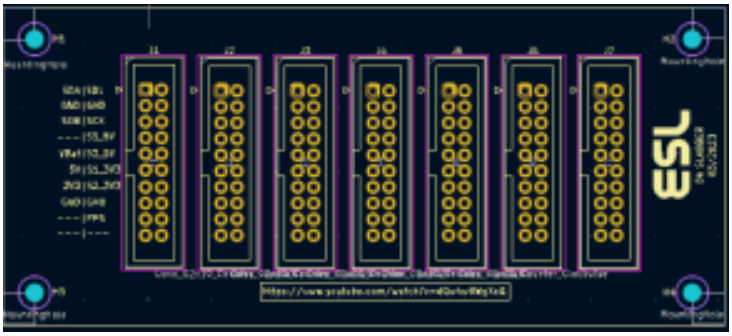

(b) PocketQube Backplane. Reproduced from [2].

Figure 2.1: PocketQube Mechanical Interface. Reproduced from [2].

Table 2.2: Backplane Pin Definitions. Adapted from [2].

Pin	Function	Pin	Function
1	SDA	11	User Defined (MOSI)
2	Ground	12	Ground
3	SDB	13	User defined
4	User defined	14	S2 5V
5	VBat	15	S1 5V
6	5V line	16	S2 3V3
7	3.3 line	17	S1 3V3
8	Ground	18	Ground
9	User defined(MISO)	19	SCK
10	PPS	20	Reset

The PocketQube is divided into subsystems, where each subsystem is developed separately usually by separate work groups according to a standard set within the group itself. This project focuses on the Electrical Power System (EPS) which provides power to the satellite. Other subsystems can include the Attitude Determination and Control System (ADCS) which stabilizes the satellite, Communication Link (COMM) with communication made possible through the ground station, On board computer (OBC) the brain of the satellite, EPS and the payload. Critical subsystems will be connected onto the 5V and 3.3V bus where non-critical subsystems will be connected onto the switched power busses which protects the EPS from damage if too much current is drawn.

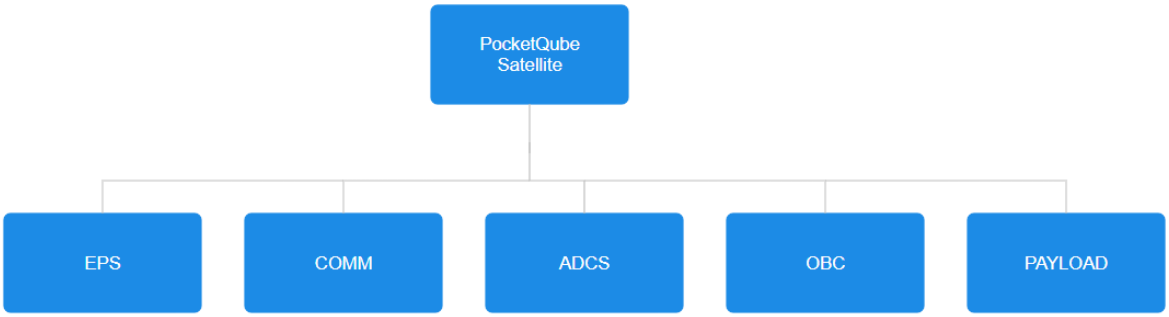

Figure 2.2: Self-derived representation of PocketQube Subsystems designed by each student within the group.

2.2. PocketQube Electrical Power System

The EPS can be further subdivided into Figure 2.3, which shows all the different components required to build a functional EPS.

The PocketQube satellite will harvest energy from sunlight by using solar cells. The harvested energy will be used to charge a Li-ion battery which will supply power to the subsystems of the PocketQube through switched regulated lines. This section will deal with

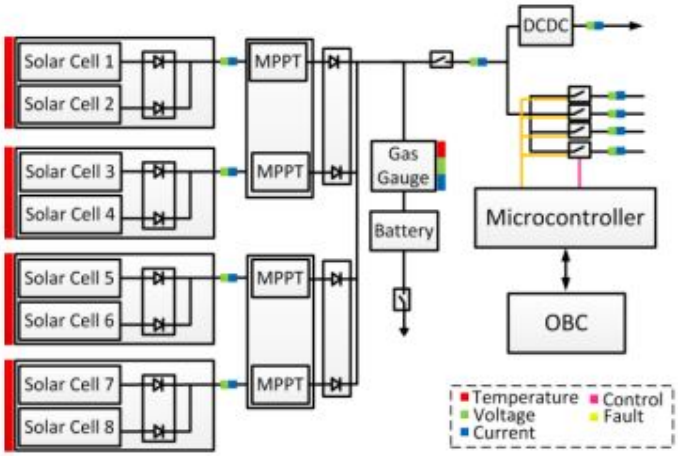

Figure 2.3: The EPS subsystem. Reproduced from [3].

the theoretical principles behind solar- to electrical energy conversion, power distribution techniques as well as theory behind rechargeable Li-ion batteries.

2.2.1. Photovoltaic cells

A solar cell is a device that converts the energy of sunlight directly into electricity via the photovoltaic effect [4]. At the heart of the photovoltaic cells is the silicon wafer. The structure of the silicon atoms consists of bonded connections with electrons that have no freedom of movement. If phosphorous atoms with five valence electrons are injected into the silicon wafer, one electron will be free to move. This is known as n-type doping. When the electrons get enough energy they will move freely. When light from the sun strike these electrons they will gain photon energy and start to move at random. However this random movement does not result in any current through a load. To make the electrons move in a single direction this structure requires some driving force.

Solar cells are commonly arranged in a large area p-n junction made from silicon which acts as the driving force for the solar cell electrons. When a p-type silicon is placed in close contact with an n-type silicon, electrons will diffuse from the n-type region with high concentration to the p-type region with low concentration and recombine with holes on the p-type region. Similarly, holes, which is created by p-type doping, will diffuse from the p-type region to the n-type region creating a diffusion current I_D in the same direction. Eventually, an equilibrium is reached where the net current is zero leaving a region with no charge carriers known as the depletion region. Due to the migration of the holes and electrons, the n-side of the depletion region becomes slightly positively charged and the p-side becomes slightly negatively charged. This electric field creates a diode with a drift current I_S which opposes the diffusion current I_D [4]. This is the necessary driving force as mentioned above.

When light hits the p-n junction and penetrates through the n-region up to the depletion

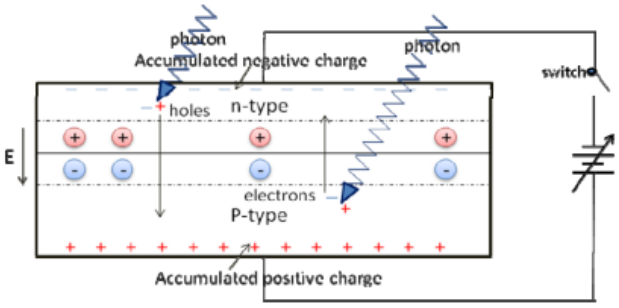

Figure 2.4: Photo-generated voltage and current. Reproduced from [4].

region, the photon energy is sufficient to generate electron-hole pairs in the depletion region. The electric field in the depletion region drives the electron-hole pairs out into the n- and p-region. Eventually the concentration of electrons in the n-region and the holes in the p-region become so high that a potential difference will develop between them. As soon as you connect a load between these two regions, electrons will start flowing through the load and reconnect with the holes in the p-region [5].

2.2.2. Solar Cell characteristics

To be able to characterize a solar cell it is useful to work with a model which is electrically equivalent. An ideal solar cell can be modeled according to Figure 2.5a which is directly derived from the theory of PV cells [4].

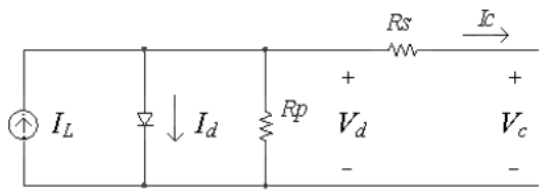

(a) Solar cell equivalent circuit. Reproduced from [4].

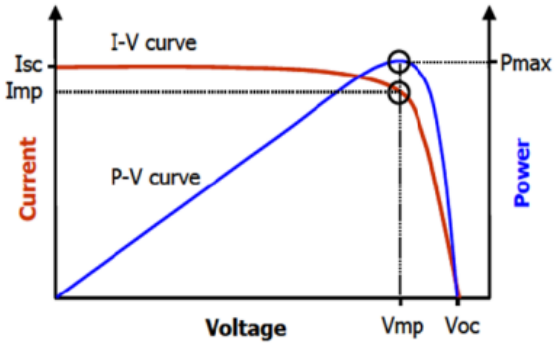

(b) Typical I-V and P-V characteristics of a PV Cell. Reproduced from [6].

This circuit can be used to model the behaviour of a solar cell and can be used effectively to make efficient designs. Characteristics of a solar cell can thus be simulated using this equivalent model which consists of output current and power versus output voltage. Figure 2.5b shows the typical characteristics of a solar cell under ideal conditions [4].

The power rises until it eventually reaches a point know as the Maximum Power Point which is the highest amount of power that the cell can generate at that current moment. A significant drop comes after the cell has reached the MPP as the panel voltage reaches

the open-circuit voltage. Ideally you would always aim to extract the MPP current, I_{mp}, and voltage, V_{mp}, to ensure maximum power delivery out of the solar cells.

Environmental or load conditions affect the operating point on the I-V curve. The need for a Maximum power point tracking (MPPT) system is evident due to changes in sunlight intensity, temperature, and load which can lead to variations in the I-V characteristics of the solar cell, causing the MPP to shift. To utilize the full potential of the solar cell an MPPT system becomes essential for maintaining efficiency and maximizing energy output at all times.

2.3. Power Regulating

One of the main challenges of a power system is the fact that a single source of power is mainly used to distribute power between different electronic components that each require different operating voltages than the voltage of the power supply. The voltage needs to either be stepped down or stepped up depending on the operating voltage of the electronic component. This is especially a problem in battery operated systems such as an EPS for a PocketQube. A circuit that can create a dc voltage higher than that of a certain source is referred to as a *step-up dc-dc* converter and one that can create a dc-dc voltage lower than that of a certain source is referred to as a *step-down dc-dc* converter. A switched-mode step up converter is called a *boost* converter and a switched mode step-down converter is called a *buck* converter. Another type of switched mode dc-dc converter is a *buck-boost* converter, which is able to step-up or step-down dc voltage of opposite polarity. [7].

2.3.1. Buck Converter

The simplest step-down converter that we all are familiar with is the resistive divider as shown in Figure 2.6

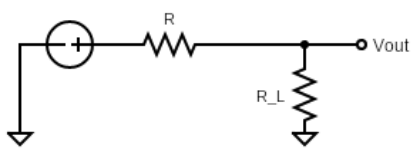

Figure 2.6: a Simple resistive divider

Where $V_{out} = \frac{R_L}{R_L+R} V_{Batt}$. Although the complexity is simple, this circuit has 2 problems. When the load current changes as a function of time a fixed resistor value R will cause a time-varying voltage across the load. The second problem is due to the fact that lets say $R = 2k\Omega$ and $R_L = 1k\Omega$, the resistor R will use twice the amount of power than the load.

Ideally we would want the most power to be delivered to the load [7]. Introducing the Buck converter.

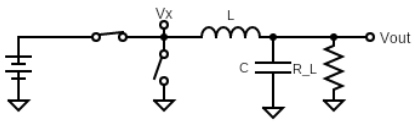

(a) Buck converter Position 1

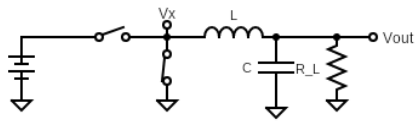

(b) Buck converter Position 2

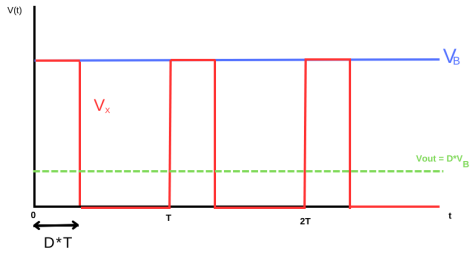

(c) Buck converter voltage waveform

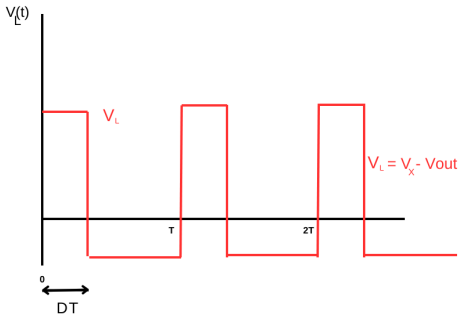

(d) Buck converter inductor voltage waveform

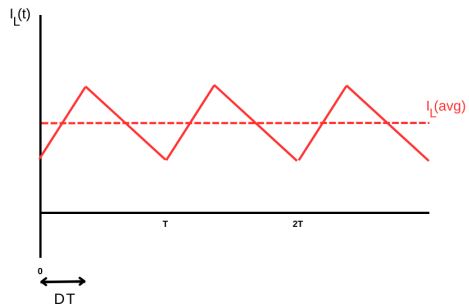

(e) Buck converter inductor current

Figure 2.7: Buck Converter

The main goal of the Buck converter is to find a weighted average between the battery voltage and 0V. By turning the battery on and off periodically with the 2 switches as shown in the Figures 2.7a and 2.7b, a periodic voltage waveform will form at the V_x node as shown in Figure 2.7c that changes between V_B and zero with a duty cycle of D. The average of this voltage can be obtained by passing it through a second order low pass filter with a cut-off frequency lower than the fundamental frequency of V_x. As a result of the low pass filter only the DC component of V_x will remain at the output, while all the other frequency components will be attenuated. This DC voltage is the average of the voltage V_x and can be rewritten as $V_{out} = D \cdot V_B$ as seen by the green plot in Figure 2.7c [7].

V_{out} is shorted to V_x at DC because of the inductor acting as a short circuit while the other frequency components will be impeded by the inductor and shorted to ground by the capacitor. The voltage across the inductor will then simply be the voltage difference between V_x and V_{out} such that the DC voltage drop (Average voltage of waveform) across the inductor is 0V as shown in Figure 2.7d. This makes sense as the impedance across the inductor is zero at DC thus its voltage should also be zero at DC. According to the

integral form of the inductor i-v equation: $i = \frac{1}{L}\int_0^T vdt + i_0$,The current through an inductor is the integral of its voltage with a proportionality constant of $\frac{1}{L}$. This results in the waveform $I_L(t)$seen in Figure 2.7e with the average current through the inductor being delivered to the load because the capacitor acts an open circuit in DC [7].

Assuming ideal switches, inductors and capacitors, the output voltage is always equal to $D \cdot V_B$ independent of R_L, as there is no series resistance or leakage through the components. The circuit also delivers all its battery power to the load. This solves both problems we faced by simply using a resistive divider and enables us to use the Buck Converter principle when facing such power problems.

2.3.2. Boost Converter

Although it is quite simple to make a linear step down regulator, it is not as simple to make a linear step up regulator. Voltage amplifiers are the best option to boost a voltage from some battery power supply but it has one problem. An amplifier typically needs a higher supply voltage than the desired output voltage. The Boost converter provides us with a switching-mode step-up converter.

The main goal of the boost converter is to create a positive voltage over the inductor, which is in series with the battery voltage. This creates a higher supply voltage with which a higher output voltage can be created. Similar to the Buck converter this converter also works with two switches in two different positions. In Figure 2.8a the battery voltage is passed across the inductor, this creates a growing magnetic flux that is the time integral of the battery voltage. [7] According to the integral form of the inductor i-v equation: $i = \frac{1}{L}\int_0^T vdt + i_0$, the inductor integrates the battery voltage to produce a current with a proportionality constant of $\frac{1}{L}$. This current waveform is similar to the Buck converter and can be seen in Figure 2.8e. The max current is reached at the end of the first position and is released into the capacitor in position 2 which creates an average current output.

When all the currents and voltages are constant we can assume steady state is reached. If the circuit is in position 2 the inductor will lose all its flux gained in position 1. If the time period it takes to flux up the inductor is $D \cdot T$, the total flux at the end of position 1 will be equal to $D \cdot TV_B$. The loss of this flux in position 2 over a time period of $(1 - D)T$ will produce a voltage of $V_B \cdot \frac{D}{1-D}$ across the inductor. The inductor is in series with the battery voltage V_B. This means a output voltage of $V_{out} = V_B + V_B \cdot \frac{D}{1-D} = \frac{V_B}{1-D}$. Regardless of the value of D, with $D < 1$, the output voltage will always be higher than the battery voltage [7].

Choosing Between Boost and Buck Converters

The choice between Boost and Buck converters depends on the application's specific requirements. Boost converters are suitable when the output voltage needs to be higher

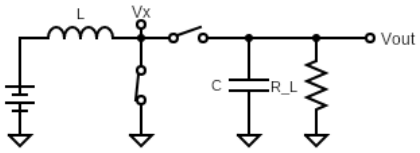

(a) Boost converter Position 1

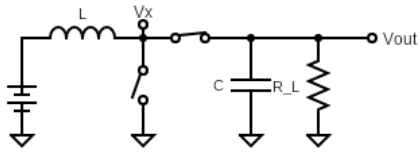

(b) Boost converter Position 2

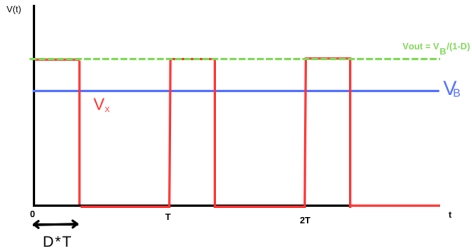

(c) Boost converter voltage waveform

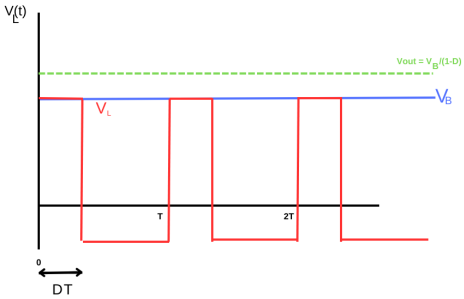

(d) Boost converter inductor voltage waveform

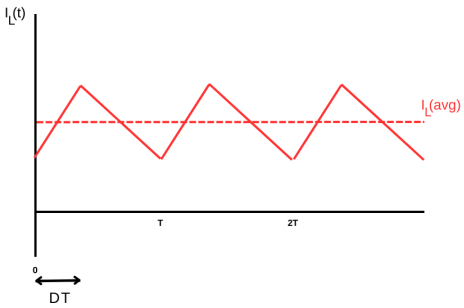

(e) Boost converter inductor current

Figure 2.8: Boost Converter

than the input voltage, making them ideal for applications where a voltage step-up is necessary. On the other hand, Buck converters are preferable when the output voltage must be lower than the input voltage, providing an efficient solution for voltage step-down applications. The selection between the two depends on the specific power management needs of the system.

2.4. Maximum Power Point Tracking techniques

The aim of MPPT is to harvest the maximum amount of power out of your Photovoltaic (PV) cells within changing conditions, by matching its I–V operating point with the load characteristic. We can utilize techniques like regulating the panels output voltage or current to operate the converter at the PV panel's MPP which in turn delivers maximum power output from the PV panel. [8].

Multiple techniques have been developed over the years that serve the same purpose but differ in aspects such as efficiency, complexity, implementation and steady state oscillation. Three techniques are commonly used within the design of an EPS for picosatellites, Perturb & Observe, Incremental Conductance and Constant Voltage [9]

2.4.1. Perturb & Observe Algorithm

The main idea behind the P&O algorithm uses the fact that on the PV-curve in Figure 2.5b there is a trend seen in the change in voltage and power towards or away from the MPP.

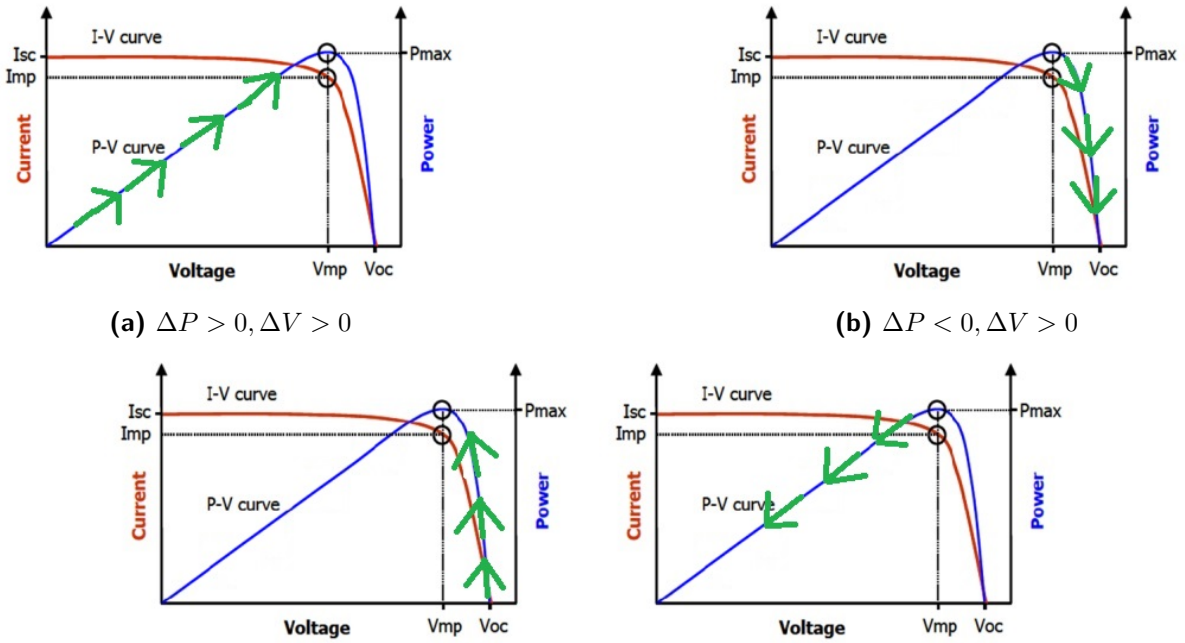

(a) $\Delta P > 0, \Delta V > 0$ **(b)** $\Delta P < 0, \Delta V > 0$

(c) $\Delta P > 0, \Delta V < 0$ **(d)** $\Delta P < 0, \Delta V < 0$

Figure 2.9: Four trends in a P-V graph for a PV cell. Adapted from [6].

By evaluating the change in power and then increasing or decreasing the PV panel's output voltage depending on this evaluation, the P&O algorithm forces the system to approach the MPP. In Figure 2.9a there is an increase in both power and voltage output thus approaching the MPP. In Figure 2.9b there is a decrease in power but an increase in voltage output thus moving away from the MPP and so the trend differs for the other

2 figures as well. These trends can be utilized along with the Pulse Width Modulation (PWM) control of the Buck/Boost Converters to either increase or decrease the output voltage to force the system to approach the MPP.

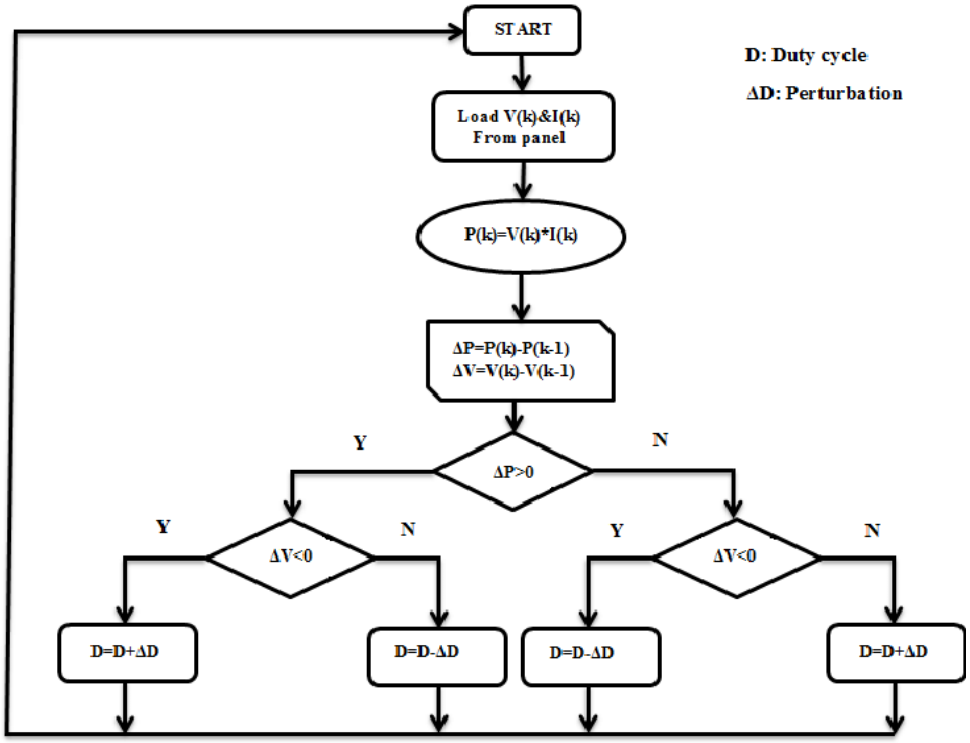

Figure 2.10: The P&O algorithm. Reproduced from [10].

The algorithm starts of by measuring the output voltage and current from the PV panel at a certain time instant. The voltage at that instant is compared to the previous time instants' voltage. The power at that instant is then calculated and compared to the previous instant. The change in power is evaluated and then the change in voltage to be either increasing or decreasing. Based on which trend is seen according to Figure 2.9, the duty cycle is increased or decreased through the microcontroller that controls the PWM controlled switch in the Boost/Buck converter. The algorithm then repeats.

2.4.2. Incremental Conductance Algorithm

The Incremental conductance algorithm is based on the fact that the slope of the panels P-V curve is zero at the MPP, positive on the left and negative on the right of the MPP [11]. The algorithm measures the instantaneous conductance ($\frac{I}{V}$) and the incremental conductance ($\frac{\Delta I}{\Delta V}$) to then determine the current slope on the PV panels P-V curve. The following relationships describe the slope of P-V curve.

$$\left\{ \begin{array}{ll} \frac{\Delta I}{\Delta V} + \frac{I}{V} = 0 & at\ MPP \\ \frac{\Delta I}{\Delta V} + \frac{I}{V} > 0 & left\ of\ MPP \\ \frac{\Delta I}{\Delta V} + \frac{I}{V} < 0 & right\ of\ MPP \end{array} \right\} \tag{2.1}$$

To address the issue from noise, measurement faults and quantization, where the condition $\frac{\Delta I}{\Delta V} + \frac{I}{V} = 0$ is rarely met, resulting in steady-state oscillations around the MPP, introduce a new parameter ϵ, defined as follows [11].

$$\left|\frac{\Delta I}{\Delta V} + \frac{I}{V}\right| \leq \epsilon \tag{2.2}$$

The magnitude of oscillations around the MPP is determined by the value of ϵ, as ϵ increases, the magnitude of oscillations decreases. For relatively large values of ϵ, the operating point deviates from the actual MPP. Therefore, the choice of ϵ should be made sensibly to optimize the performance of the MPPT system [11].

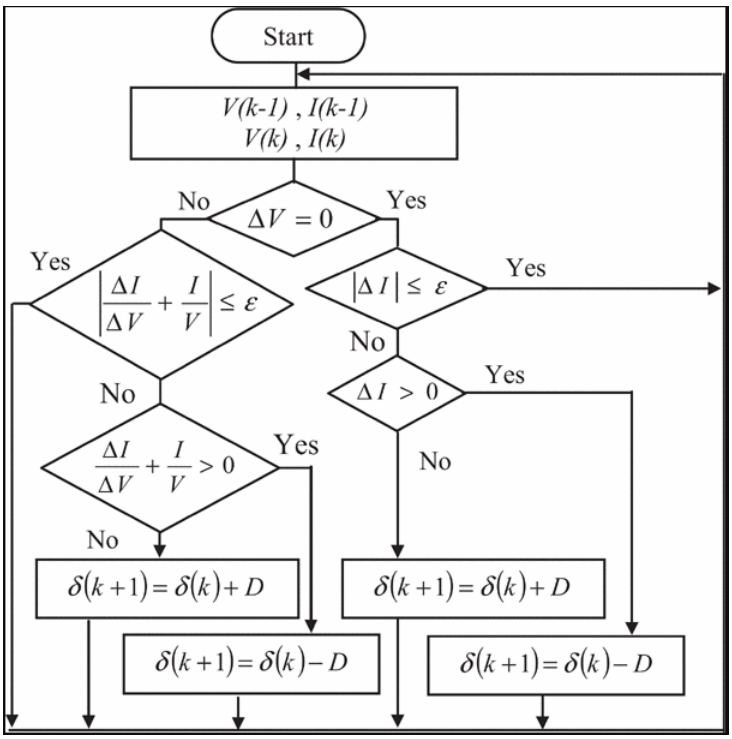

Figure 2.11: Incremental Conductance. Reproduced from [11].

The algorithm starts by measuring both the present and previous output voltage and current values from the PV panel. It then calculates the incremental conductance ($\frac{\Delta I}{\Delta V}$). Based on the measured conductance values, the algorithm evaluates the slope conditions to identify the relative position of the operating point on the P-V curve. The algorithm operates in an iterative manner, continuously measuring and calculating the incremental conductance and adjusting the PV panel's voltage accordingly.

2.4.3. Constant Voltage Algorithm

The Constant voltage algorithm regulates the solar array voltage according to a fixed reference voltage which is the assumed MPP of the solar cell array. The algorithm is simple and easy to implement. The solar array voltage is measured, compared to the

reference voltage and the difference between the two is used to drive a power conditioner, such as a voltage regulator with some power improvement functions. This method fixes the voltage very quickly as it requires very little computation.

This might sound good but the method comes with some issues. It doesn't take in the fact that the solar arrays I-V characteristics vary within different conditions such as temperature, wear and irradiation differences. These varying conditions cause a shift in the voltage at the MPP. The constant voltage algorithm would then deliver an inaccurate MPP because of this change.

MPPT Selection

The Perturb & Observe (P&O) algorithm stands out as a powerful and widely adopted choice for MPPT. Several factors contribute to its preference in the context of energy harvesting from photovoltaic cells:

- Simplicity and Ease of Implementation: The P&O algorithm is straightforward to implement, making it an attractive choice for applications with limited computational resources, common in small satellites such as PocketQubes.
- P&O adapts in real-time to changing environmental conditions by continuously adjusting the operating point based on the observed trends in voltage and power.
- The P&O algorithm integrates with PWM control strategies.

These features make the P&O algorithm the suitable option for the energy harvesting system in this project.

2.5. Battery Management Systems

Batteries are the main energy source for the PocketQube during eclipse periods or when peak power is required. This section reviews the principles behind lithium-ion (Li-ion) batteries which are commonly used in spacecraft [12].

2.5.1. Lithium Ion Batteries

Li-ion batteries have high energy density and rechargeable capabilities. Figure 2.12 shows the energy densities of different types of batteries compared to Li-ion batteries. It is clear that the Li-ion batteries are top choice when looking for batteries with a high size to energy ratio.

A Li-ion cell typically consists of an anode and cathode which are the negative and positive electrodes. They are then connected by an electrolyte, typically liquid, polymer gel and ceramic, containing lithium ions. The electrodes are isolated by a separator, which

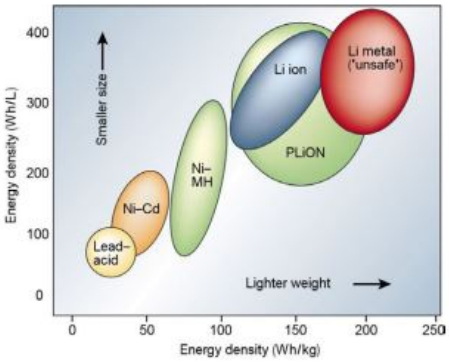

Figure 2.12: Energy Densities of different battery types. Reproduced from [13].

only allows the flow of lithium ions between the electrodes and not electrons. Connecting the two electrodes to an external electrical supply causes the electrons to be released from the cathode and then moved through the supply to the anode. At the same time lithium ions flow internally through the electrolyte from cathode to anode. This allows the external electrical energy to be stored in the form of chemical energy in the anode and cathode, therefore charging the battery. Connecting an external load to the electrodes causes the opposite reaction to the charging process. Electrons now move from the anode to the cathode through the load and lithium ions follow the same direction within the electrolyte. The electrochemical reactions at the two electrodes releases the stored chemical energy. therefore discharging the battery. Figure 2.13 shows the working principle behind charging and discharging within the battery.

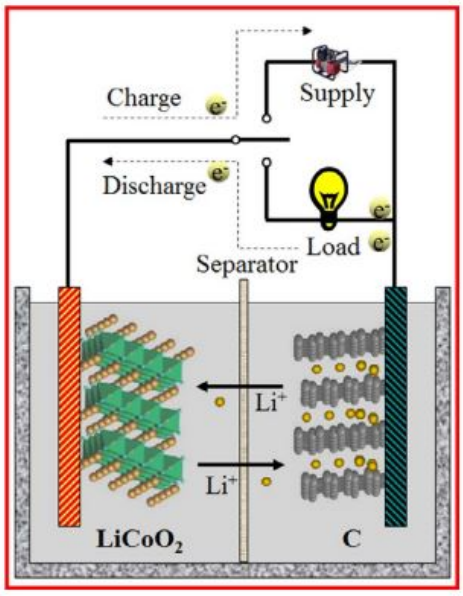

Figure 2.13: Electrochemical composition of a li-ion battery. Reproduced from [13].

The characteristics of li-ion batteries are determined by a number of important parameters which serve critical in performance analysis.

- **Energy Density (Wh/kg)**: The amount of energy that can be stored and released per unit mass.
- **Capacity (Ah)**: The amount of energy that can be stored within the battery.
- **C-rate:** A measure of the rate at which a battery is charged or discharged relative to its capacity.
- **Depth of Discharge (DOD):** The percentage of a battery's capacity that has been discharged concerning its total capacity.
- **State of Charge (SOC):** The current level of charge in a battery, expressed as a percentage of its total capacity.

2.5.2. Battery charging methods

Constant Current (CC)

The battery is supplied with a current at a constant value, typically at 1C, 0.5C, or as specified by the battery supplier. During the charging process, the supply voltage varies to maintain a constant current. However, a challenge arises in achieving a full 100% SOC without causing damage to the battery. As the battery charges, its voltage increases. The voltage across the battery terminals is limited by the battery chemistry. In constant current mode, the voltage continues to rise until it reaches a predefined voltage limit [14].

Constant Voltage (CV)

A constant voltage at the maximum voltage of the battery with current limited to the maximum capacity of the battery or otherwise, is applied to the battery terminals. The charge current is high at first and then slowly decreases over time as the battery charges. The only disadvantages of this method is the high current at the start and temperature increase. The method also takes longer to charge as the charge current decreases over time [14].

Constant Current Constant Voltage(CCCV)

Constant Current Constant Voltage (CCCV) charging combines the initial CC phase, where the battery is supplied with a constant current, with the CV phase, where a maximum voltage is applied while the current decreases. As shown in Figure 2.14, the charging process starts with a controlled current usually, 0.1C for trickle charging if the battery is deeply discharged and 0.5C-1C for CC, allowing the battery voltage to rise until it reaches a predetermined limit, at which point the charger switches to a CV mode, ensuring a

gradual and controlled approach to reaching a full 100% SOC without causing damage to the battery [14].

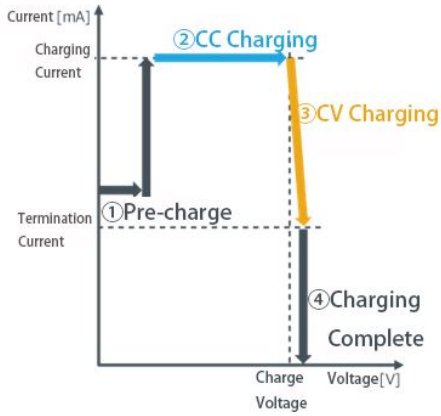

Figure 2.14: CCCV algorithm. Reproduced from [15].

Charging Method Selection

Choosing the appropriate charging method is crucial for BMS. Among the various charging methods, CCCV stands out as the preferred choice for several reasons:

- Gradual Charging: CCCV allows for a controlled and gradual increase in voltage, reducing the risk of damage to the battery, particularly when approaching a full 100% SOC.
- Flexible Charging Rates: The initial constant current phase in CCCV accommodates both trickle charging and higher current charging based on the battery's state, providing flexibility in adapting to different charging scenarios.
- Temperature Control: CCCV helps in controlling temperature rise during charging compared to methods with high initial currents, contributing to the overall safety and longevity of the battery.

Considering these factors, CCCV emerges as a well-balanced charging method suitable for the unique requirements of BMS in the PocketQube.

Chapter 3: Detail Design

3.1. System Diagram

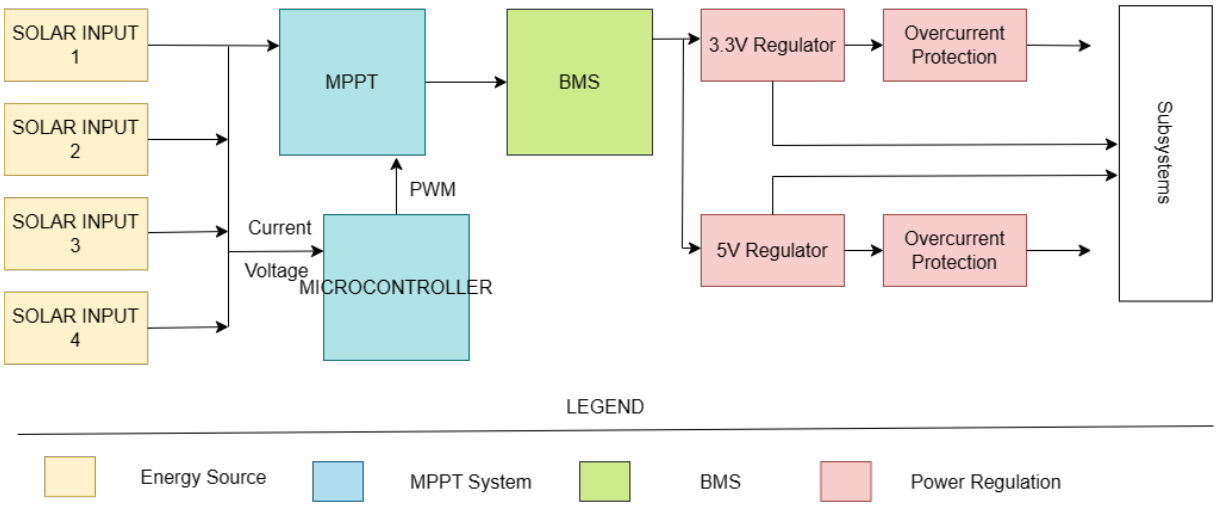

Figure 3.1: Proposed EPS subsystem

The proposed EPS subsystem, illustrated in Figure 3.1, is designed based on insights gained from the literature review on MPPT techniques, battery management methods and power regulation.

The subsystem comprises key elements to ensure efficient power management and energy storage. The MPPT techniques, such as P&O are integrated to maximize power extraction from the PV cells under varying environmental conditions.

To store solar energy, the subsystem includes a battery charging system with a CCCV charging algorithm and battery protection.

Boost and Buck converters are implemented into the design. The Boost converter steps-up voltage when necessary. The Buck converter steps down the voltage when needed. The selection between Boost and Buck converters is made based on the specific power management requirements of the system, as outlined in the literature.

Overcurrent protection circuits protects the EPS in the case of too much current or short circuits in the downstream subsystems.

3.2. MPPT

The primary goal of the MPPT design is to efficiently extract power from the solar cell arrays and regulating it for the BMS using the LTC3130-1 Boost-Buck converter. The LTC3130-1 is chosen due to its high efficiency, which is ideal for space applications where energy isn't easily obtainable. The desired characteristics for the LTC3130-1 are summarized further in Table C.1 in Appendix C

3.2.1. Hardware

The design of the LTC3130-1 closely adheres to the typical application circuit, in Figure 3.2 and information outlined in the LTC3130-1 datasheet [16]. This ensures that the system uses the manufacturer's recommended configuration for optimal performance and reliability.

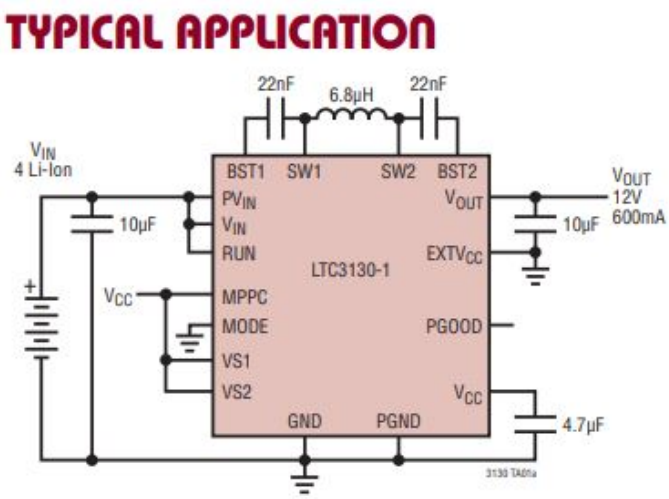

Figure 3.2: LTC3130-1: Typical Application. Reproduced from [16].

The application circuit and its components have been modified to achieve the desired outputs using the applications information, from the datasheet, as a guideline.

The LTC3130-1 has an MPPC function that optimizes performance when operating from solar cells. The pin can be used to adjust the inductor current in order to maintain a minimum input voltage as set by the voltage at the MPPC pin.

Referring to Figure 3.3, the MPPC pin is connected to a non-inverting input of a g_m amplifier, whose inverting input is connected to a 1V reference. When the voltage on the MPPC pin drops below the reference voltage the amplifier pulls the VC node to ground. This reduces the average inductor current which reduces the input current and regulates V_{IN} to the programmed minimum voltage. It is recommended on page 21 in the datasheet to use an external voltage divider to set the minimum input voltage from the panels according to the following formula, $V_{IN(MPPC)} = 1.00V \cdot (1 + \frac{R5}{R6})$ [16]. However a different

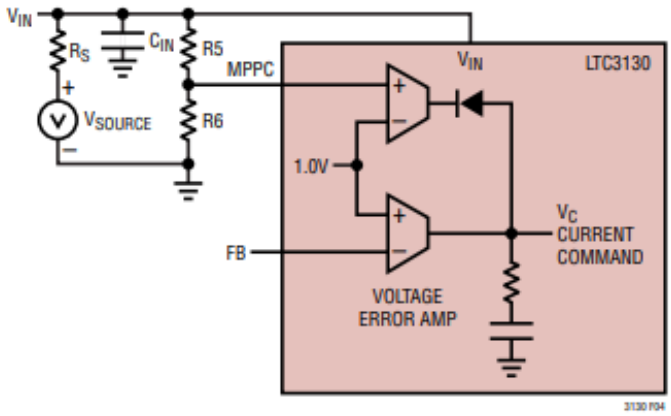

Figure 3.3: MPPC amplifier with external resistor divider. Reproduced from [16].

approach will be used. The idea is to send an analog voltage from the microcontroller using PWM that sets the MPPC pin accordingly using sensors to maximise the MPP. The aim is to have a more accurate measurement and use of the MPP instead of using an ”estimated” MPP to regulate the input voltage.

The LTC3130-1 has an internal voltage divider that can be utilised to program the output voltage, V_{OUT}, to a constant voltage. This can be programmed by the VS1 and VS2 pin according to the one of four fixed voltages as seen in Table 3.1. The output voltage will be programmed to a constant 5V to allow easier integration into the battery charging IC's input voltage.

Table 3.1: Program settings for V_{OUT} in LTC3130-1. Reproduced from [16].

VS2	**VS1**	V_{out}
0	0	1.8V
0	V_{CC}	3.3V
V_{CC}	0	5.0V
V_{CC}	V_{CC}	12V

The inductor and decoupling capacitors are all standard values from the application circuit in Figure 3.2. The final schematic was based on the formulas and instructions provided above and in the datasheet, and in Appendix E, Schematic page 6.

3.2.2. Software

The software design for the P&O algorithm is implemented on the ATmega328P microcontroller, with desired characteristics in Table C.2 in Appendix C. This algorithm aims to dynamically adjust the voltage on the MPPC pin of the LTC3130-1 in response to changes in solar panel conditions, ensuring maximum power point tracking.

The P&O algorithm operates based on the principle of perturbing the operating point and observing the change in power to determine the direction towards the MPP. The

algorithm uses current sensors for measuring the panel current (I_{in}) and an ADC for measuring the panel voltage (V_{in}).

1. **Initialization:** Initialize ADC, PWM, and other necessary peripherals. Set the initial PWM duty cycle to a nominal value.
2. **Read Measurements:** Periodically read current (I_{in}) and voltage (V_{in}) from the respective sensors.
3. **Calculate Power:** Use the obtained current and voltage measurements to calculate the input power ($P_{\text{in}} = I_{\text{in}} \times V_{\text{in}}$).
4. **Compare Power:** Compare the calculated power (P_{in}) with the previously measured power. Determine if there is an increase, decrease, or no change.
5. **Adjust PWM Output:**
   - If power increases, increment the PWM duty cycle to perturb towards higher power.
   - If power decreases, decrement the PWM duty cycle to perturb towards lower power.
   - If no change in power, maintain the current PWM duty cycle.
6. **Store Previous Measurements:** Save the current measurements (I_{in}, V_{in}, P_{in}) for future comparisons.
7. **Repeat:** Repeat the process in a closed-loop fashion.

PWM Output and RC Filter

The PWM signal generated by the ATmega328P is filtered using an RC filter before being applied to the MPPC pin of the LTC3130-1. The PWM output is adjusted based on the P&O algorithm's decision to perturb towards the MPP.

Integration with External Sensors

The microcontroller interfaces with external sensors for current and voltage measurements. The analog voltage from the current sensors is converted to a digital value using the microcontroller's ADC. The panel voltage is directly measured using the ADC.

Code Structure

The software code is structured according to Appendix F to manage the P&O algorithm, ADC readings, PWM generation, and sensor interfacing. The main loop continuously executes the P&O algorithm, adjusting the PWM output to dynamically track the maximum power point.

3.2.3. MPPT Experimental Design

Objectives:

- Assess the performance of the LTC3130-1 in regard to MPPC functionality for solar charging applications.
- Evaluate the efficiency of the LTC3130-1 buck-boost converter under various load conditions.

Setup:

- Connect a solar energy source to the input of the LTC3130-1.
- Use the Atmega328 microcontroller's PWM capability along with the Perturb and Observe algorithm to adjust the MPPC pin voltage according to sensor measurements from the solar panels' output.
- Connect the LTC3130-1's MPCC pin to the Atmega328 via a low-pass filter, to convert the PWM output to a DC voltage for MPPC.
- Connect a varying load to the output pin of the LTC3130-1.

Procedure:

- Program the Atmega328 microcontroller to output a variable PWM signal according to the P&O algorithm.
- Connect the PWM output to a low-pass filter to convert it to a DC voltage.
- Connect the output of the low-pass filter to the MPPC pin of the LTC3130-1.
- Connect the energy source, such as a solar panel, to the input of the LTC3130-1.
- Use multimeters to monitor both the input voltage (solar panel output) and output voltage (LTC3130-1 output) in real-time.
- Measure the input/output current under different load conditions.

- Adjust the duty cycle of the PWM and observe the impact on the output voltage and current.
- Record all findings and graph the performance of the buck-boost converter under changing conditions.

3.3. Battery Management System

The LTC4066 is an integrated linear charger and ideal diode for single-cell Li-ion or Li-polymer batteries. It is designed to work with wall adapter power supplies or a USB power source.

In this section, a design that uses the LTC4066 IC, with characteristics specified in Table C.4 in Appendix C, to charge a 3.7V Li-ion battery using a constant 5V input from the design in section 3.2 will be presented along with a battery protection unit to prevent overcharging, overdischarging, overvoltage, undervoltage and shortcircuiting using the BQ29700 with characteristics specified in Table C.7 in Appendix C.

3.3.1. Battery Charging

The battery charging algorithm with CCCV from LTC4066 is ideal for Li-Ion batteries. The charger will first apply a constant programmed current to the battery until it reaches a specified voltage limit, approximately 4,1V, then switch to a constant voltage mode and reduce the charging current until the battery is fully charged [17]. The design of the LTC4066 closely adheres to the typical application circuit, in Figure 3.4, and information outlined in the LTC4066 datasheet [17].

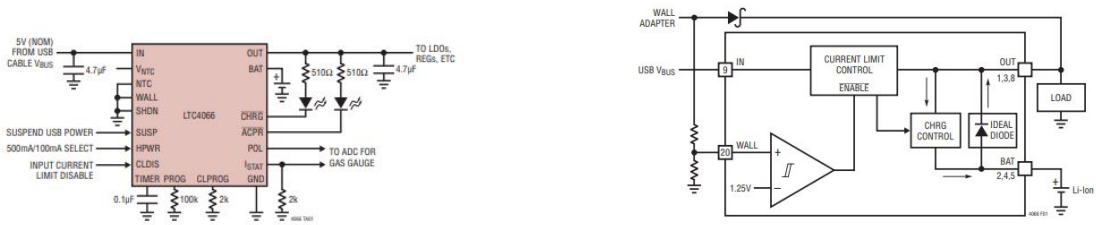

Figure 3.4: LTC4066: Typical Application and Simplified Block Diagram. Reproduced from [17].

The 5V supply input from the LTC3130-1 is connected to pin IN along with a decoupling capacitor. The IN pin has a programmable current limit. The battery charge current will be adjusted to ensure that the sum of the charge current and load current does not exceed the programmed input current limit. However we can disable this function by pulling the CLDIS pin high, which maximises the input current limit to 2.6A. In Figure 3.4 the block diagram shows an ideal diode between the BAT and OUT pin provides power

from the battery when the output/load current exceeds the input current limit or when input power is removed. By routing power through the ideal diode instead of connecting the load directly to the battery, allows a fully charged battery to remain fully charged until an eclipse is present where the external power from the solar cells wont be present. Once external power is removed, the output drops until the ideal diode is forward biased. The forward biased ideal diode will then provide the output power to the load from the battery. Additionally, powering loads that utilize switching regulators like in this case from the OUT pin instead of directly from the battery has the advantage of reducing battery charging times. This is because switching regulators typically require a consistent input power supply. When this power is drawn from the higher voltage available at the OUT pin, rather than the lower voltage at the BAT pin, the current consumption by the switching regulator is reduced. This, in turn, leaves more current available for charging the battery, resulting in shorter battery charging times.

The Li-ion battery should be connected to the BAT pin which provides the charge current. The charging current rate can be controlled using the PROG (pin 2) pin. The charging current is programmed by placing a resistor (RPROG) between the PROG pin and GND where, $R_{PROG} = \frac{50000}{I_{CHG}}$, from page 15 [17]. The IC has an internal P-channel power MOSFET and uses a CCCV charge algorithm. The charge cycle starts when the OUT pin voltage rises above the UVLO level, 3.8V typically, and the battery voltage is below the recharge threshold. If the battery voltage is below 2.8V, the charger goes into trickle charging mode until the voltage level is safe for the fast CCCV mode above 2.8V. The charge current decreases as the battery approaches the final float voltage until it eventually switches to CV charging mode

3.3.2. Battery protection

The BQ29700 IC from Texas Instruments is a battery protection system intended for 1-4 cell Li-ion and LiPo battery packs. The design of the BQ29700 closely adheres to the typical application circuit, in Figure 3.5, and information outlined in the BQ29700 datasheet [18].

The BQ29700 provides several features critical for battery safety, including:

- Overvoltage/Overcharge Protection (OVP): Prevents the cell voltage from exceeding predefined thresholds, which could cause damage to the battery and reduce its life significantly.

- Undervoltage/Over-Discharge Protection (UVP): Prevents the cell voltage from dropping below a certain threshold, a state which can also harm the battery and reduce its capacity.

- Overcurrent Protection (OCP): Ensures that the current drawn from the battery

never exceeds a preset level, preventing the battery from overheating and potentially experiencing thermal runaway.

- Short-Circuit Protection (SCP): Detects a short circuit in the downstream circuit and disconnect the battery from the load.

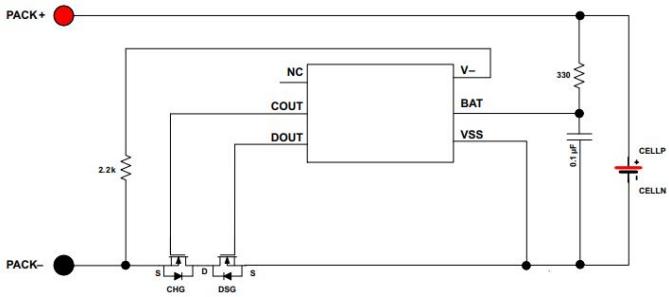

Figure 3.5: BQ29700: Typical Application. Reproduced from [18].

The design parameters for the typical application circuit in Figure 3.5 are listed in Table C.7 along with a functional block diagram in Figure C.1 in Appendix C. The BQ29700 can be interfaced using two control input signals (DISCHG and CHG Logic Inputs) to control charging and discharging switches. The FET selection for this application is important to ensure the design fulfills requirements. The datasheet recommends the CSD16406Q3 FET for the application. An RC filter on the BAT pin eliminates noise.

The functionality of the IC is as follows, referring to Figure C.1.

- **Overcharge**: The Overcharge status is detected when the battery voltage exceeds the overcharge detection threshold during the charging process. If this condition persists for a duration exceeding the overcharge detection delay, the COUT output signal is driven low, disabling the charging FET to prevent further battery charging.

- **Over-discharge**: The Over-Discharge status occurs when the battery voltage falls below the over-discharge detection voltage for a duration greater than the over-discharge detection delay. In this state, the DOUT output is set to a low state, turning off the discharge FET to prevent further battery discharge.

- **Overcurrent**: During normal battery operation, if the voltage at the V– pin falls below the charge overcurrent detection voltage due to high charge current for a duration greater than the charge overcurrent detection delay, the COUT pin is pulled low, turning OFF the charge FET and preventing further charging.

- **Short-Circuit**: The BQ29700 uses a control input signal to detect and respond to short circuits in the downstream circuit. When a short circuit is identified, the BQ29700 swiftly disconnects the battery from the load, preventing further damage and ensuring the safety of the overall system.

The final schematic was based on the formulas and instructions provided above and in the datasheet, in Appendix E, Schematic page 8, 9.

3.3.3. BMS Experimental Design

Setup:

- Connect the LTC4066 and BQ29700 in a breadboard or PCB according to the design above.
- Connect a constant voltage power source to the ”IN” pin of the LTC4066 or use the EXT USB power source.
- Ensure all connections are done properly and pins routed correctly.

Load the Battery:

- Connect the 3.7V Li-Ion Battery to the ”BAT” pin of the LTC4066.
- Ensure that the battery is connected correctly to avoid any damage.

Initial Measurement:

- Before powering up your circuit, measure the initial voltage of your battery using a multimeter.

Voltage Measurement:

- Measure the voltages at specific pins.
- Important pins to measure:
    1. The input voltage pin (IN). Given a 5V input power, the IN pin should measure close to this value (5V).
    2. The output pin (OUT). It should be controlled internally to either output the battery power or input power.
    3. The Battery Voltage

Current Measurement:

- With a Li-ion battery connected to the IC’s output, measure the current flowing into the battery from the ”BAT” pin.
- The current can be measured using a multimeter in current mode in series with the battery.

Battery Charging Test:

- Connect the IC to a partially discharged 3.7V Li-ion battery.
- Let the IC charge the battery for some time.
- Measure the voltage of the battery. It must be more than its initial voltage, indicating that the IC is indeed charging the battery.

Protection tests:

- **Input Voltage Range Test:**
  - Vary the input voltage supplied to the LTC4066 within its specified range.
  - Check if the IC responds correctly to changes in input voltage and maintains proper charging and regulation.
- **Battery Overcharge Protection Test:**
  - Apply an overvoltage condition to the battery being charged.
  - Ensure that the LTC4066 and BQ29700 activates its overcharge protection mechanism to prevent damage to the battery.
- **Battery Under Voltage Protection Test:**
  - Test the LTC4066 and BQ29700's ability to detect and respond to battery undervoltage conditions.
  - It should disconnect the battery if it falls below a safe threshold.
- **Short-Circuit Protection Test:**
  - Introduce a short circuit in the battery output.
  - Verify that the LTC4066 and BQ29700 promptly detects the fault and disconnects the output to prevent damage.
- **Battery Discharge Test:**
  - After the battery is fully charged, discharge it using an appropriate load.
  - Monitor the discharge characteristics and ensure that the battery discharges safely.
  - The LTC4066 should not attempt to recharge it immediately.
- **Efficiency Measurement:**

- Measure the efficiency of the LTC4066 by comparing input power to output power when charging the battery.
- Calculate the efficiency under different load and input voltage conditions.

3.4. Voltage Regulation

3.4.1. Regulated 3.3V

The PocketQube requires a constant 3.3V rail to deliver power to its different subsystems. The LTC3130-1 is re-used in the same configuration as Figure 3.2 however the 3.3V programmable output voltage setting in Table 3.1 is used by connecting the VS1 pin to VCC and the VS2 pin to GND. The MPPC function is not used and is thus connected to VCC as the datasheet suggests on page 11. The input voltage pin is connected to the bus voltage from the battery or solar cells depending on the states of the LTC4066. The final schematic was based on the formulas and instructions provided above and in the datasheet, and in Appendix E, Schematic page 10.

3.4.2. Regulated 5V

The PocketQube also requires a constant 5V rail to deliver power to its different subsystems. The MP3414 is a high-efficiency, synchronous, current–mode, boost converter. The typical application circuit in Figure 3.6 is used as a guide for the final application. The final schematic was based on the formulas and instructions provided above and in the datasheet, and in Appendix E, Schematic page 11.

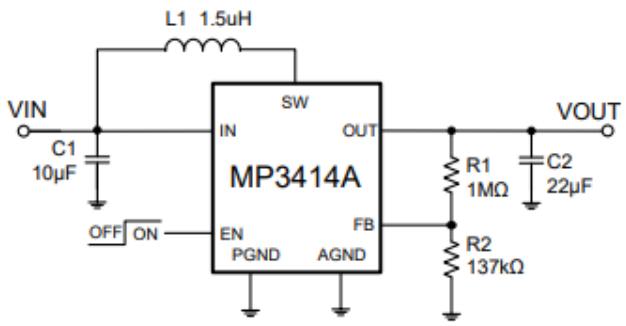

Figure 3.6: Typical Application for MP3414. Reproduced from [19].

The external voltage divider on the OUT and FB pin programs the output voltage according to page 12 in the datasheet, $V_{OUT} = 0.6V \cdot (1 + \frac{R1}{R2})$ [19]. The datasheet suggest to pick R1 and R2 as large as possible to have a lower quiescent current. Picking $R1 = 1M\Omega, V_{OUT} = 5V$ gives $R2 = 137k\Omega$. The input voltage pin is connected to the bus voltage from the battery or solar cells depending on the states of the LTC4066.

3.4.3. Regulators Experimental Design

Setup:

- Prepare power supply with the corresponding input voltages as specified in the respective datasheets for both the LTC3130-1 and the MP3414A.
- Connect a heavy, light and no load to the output and evaluate the characteristics of the regulators.

Initial Measurements:

- Individually, power each regulator and take note of the output under different load conditions.
- Examine the output voltage and current and how efficiently these converters operate at different input conditions.

3.5. Overcurrent Protection

3.5.1. Switches

Each of the subsytems connected through the switched lines on the backplane is buffered by an overcurrent protection circuit.

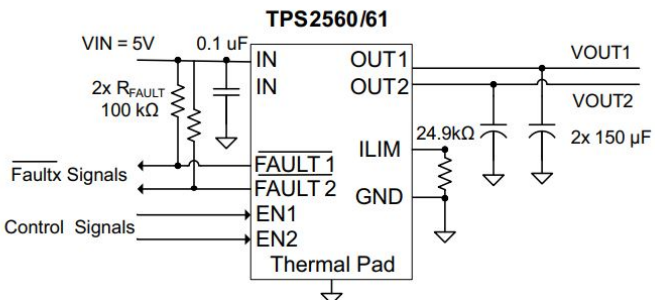

Figure 3.7: TPS2561: Typical Application. Reproduced from [20].

The TPS2561 is based on two 44mΩ high-side N-channel MOSFETS that is driven with an internal charge-pump. The typical application circuit and information in Figure 3.7 is used as a guide for the final application [20].

The TPS2561 offers a programmable current-limit threshold, ($I_{OS_{MAX}}$), between 250 mA and 2.8 A. The current-limit is programmable via an external resistor, R_{ILIM}, given by [20]:

$$I_{OS_{MAX}} = \frac{52850V}{R_{ILIM}^{0.957} k\Omega} \tag{3.1}$$

When a overcurrent/short circuit is detected the FAULT logic output is pulled low until it is fixed, and the voltage line is switched of to the subsystem via the switch [20].

The EN signal regulates the device's power supply current and supports TTL and CMOS levels, enabling a microcontroller to selectively activate or deactivate individual subsystems as needed. Combining this with a current sense circuit allows for both automated and manual detection of overcurrent using a microcontroller [20].

3.5.2. Current sensing

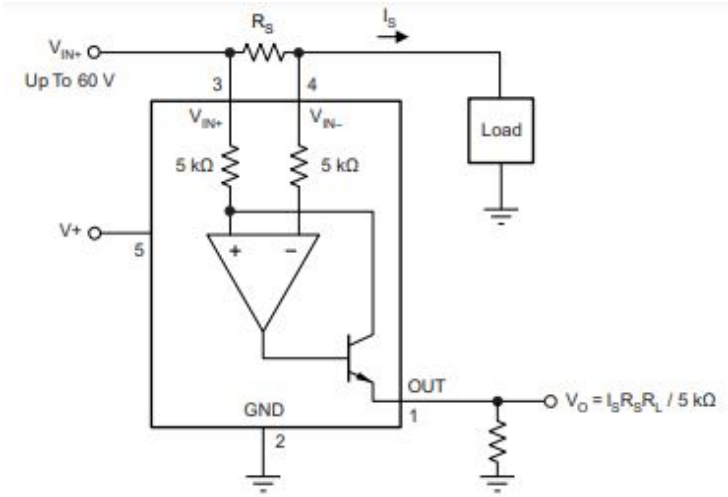

Figure 3.8: INA138: Typical Application. Reproduced from [21].

For monitoring the current consumption of each subsystem, the INA138 is used. This unipolar high-side, current shunt monitor has high gain, which allows for a small current sense resistor to minimize losses. A 50mΩ sense resistor was selected. Considering a 2A and 300mA upper limit specified by TPS2556 and a maximum microcontroller ADC voltage of 2V, the required value for RL is calculated as follows: [22]

$$R_{L5V} = \frac{V_o \cdot 5k\Omega}{R_S \cdot I_S} = \frac{2V \cdot 5k\Omega}{50m\Omega \cdot 2A} = 100k\Omega$$

$$R_{L3.3V} = \frac{V_o \cdot 5k\Omega}{R_S \cdot I_S} = \frac{2V \cdot 5k\Omega}{50m\Omega \cdot 300mA} = 667k\Omega$$

The high side overcurrent protection circuit can then be designed according to Figure 3.9 and connected before each of the switched bus lines on the backplane.

The final schematic was based on the formulas and instructions provided above and in the datasheet, and in Appendix E, Schematic page 13.

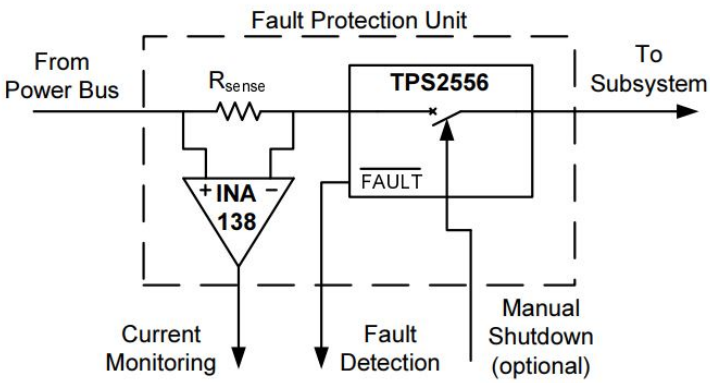

Figure 3.9: Integrated Current sensor circuit. Reproduced from [22].

3.5.3. Overcurrent Protection Experimental Design

Circuit Connection:

- Connect the input power source to the TPS2561's IN pin, and the load to the OUT pin.

Current Sensing:

- Connect the INA138 across the shunt resistor which will measure the voltage drop across this resistor. The INA138 converts this voltage to an output voltage directly proportional to the measured current.
- Feed the voltage into the ADC of the microcontroller to be able to analyse the current readings.

Overcurrent Protection:

- Automatic: Attaching a load of 2A or 300mA that draws too much current or simply shorting the line would result in the TPS2561 disconnecting the power to the load.
- Manual: The output of the INA138 is fed back to a microcontroller. The microcontroller compares the output from the INA138 to a predetermined voltage level that corresponds to the current limit. If the output is above this level, it sends a control signal to the TPS2561 to disconnect the load, thereby protecting the circuit from overcurrent.

3.6. PCB Design

A single prototype PCB was designed and brought to realization. All aspects of the PCB work, spanning from net list and schematics to wiring board design and final post-

processing, were done using the CAD software KiCad. The manufacturing process was carried out through JLCPCB.

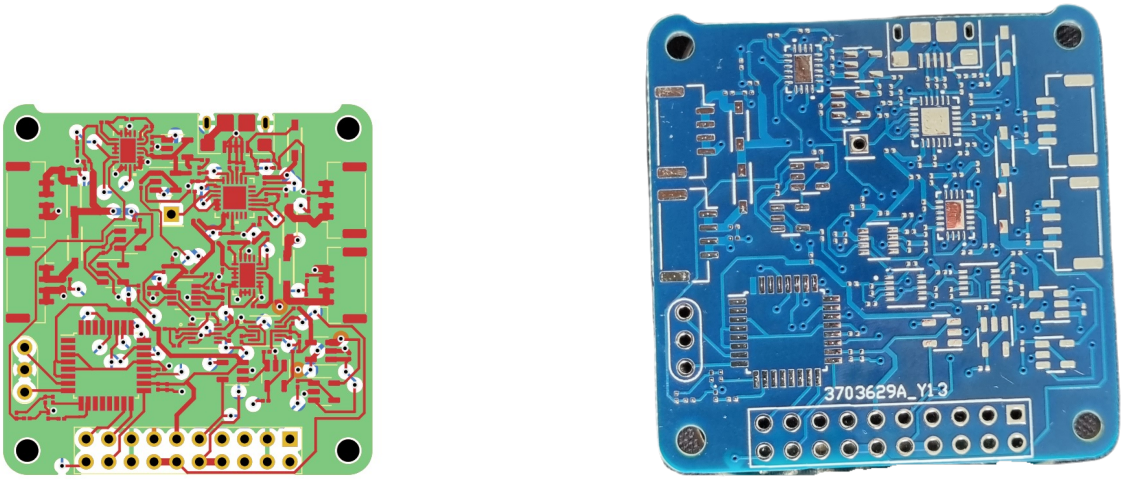

Figure 3.10: PCB Prototype 1

The first prototype shown in Figure 3.10 was realized on a four-layer board. It consisted of all the above designed circuits except for the battery protection circuit for the BQ29700 which had to be built separately due to space constraints. Alternatively a battery which contains a built-in protection circuit PCB was ordered which would integrate better with the first prototype. The PCB's dimensions were designed in accordance with the PQ9 standard as shown in Figure 2.1

The board is a standard FR4 type, with four layers. The front and bottom layers being signal layers and the two inside layers being the ground and 3.3V power planes. The physical constraints were according to JLCPCB's set constraints on their website. This prototype allowed various testing of the designed components above as well as identifying any flaws in the designs.

Chapter 4: Experiments and Results

4.1. Regulators

Expectations

The LTC3130-1 component is designed to operate in Burst Mode, a feature that significantly enhances its efficiency, especially under light-load conditions, page 12 [16].

The LTC3130-1 is configured to output a voltage of 3.3V, page 12 [16]. The typical characteristics of the LTC3130-1 in Burst Mode are graphically represented in Figure 4.1, providing insights into its behavior and performance under varying load conditions.

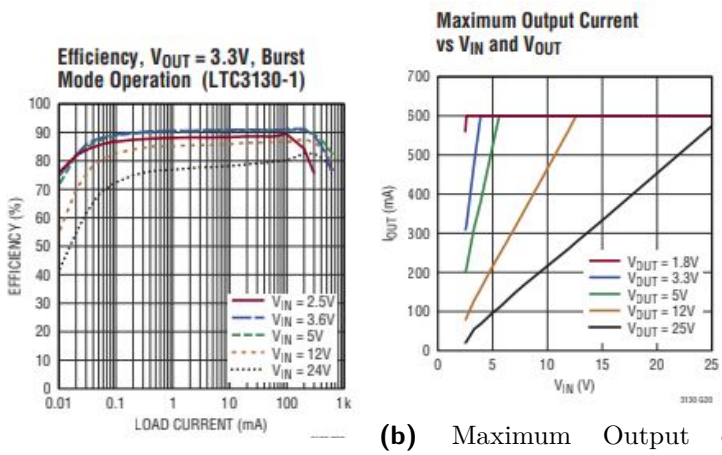

(a) Efficiency of LTC3130-1 [16] **(b)** Maximum Output of LTC3130-1 [16]

Figure 4.1: LTC3130-1: Typical Characteristics. Reproduced from [16].

Due to an ordering mistake, the originally intended MP3414A regulator was not received, and instead, the MP3414 was received. While the MP3414 and MP3414A share similarities, there are distinct differences in their characteristics. Due to limited components available at the time the design had to be altered to deliver 3.63V instead of 5V according to a different formula, $V_{OUT} = 1.21V * (1 + \frac{R1}{R2})$, page 10 [23], where $R1 = 1M\Omega$ and $R2 = 500k\Omega$. Although the specification of 5V is not met, the idea is that the layout of the 2 components are identical and that if the MP3414 works according to design, it is expected that the MP3414A will also work according to the design. The expected typical characteristics are shown in Figure 4.2.

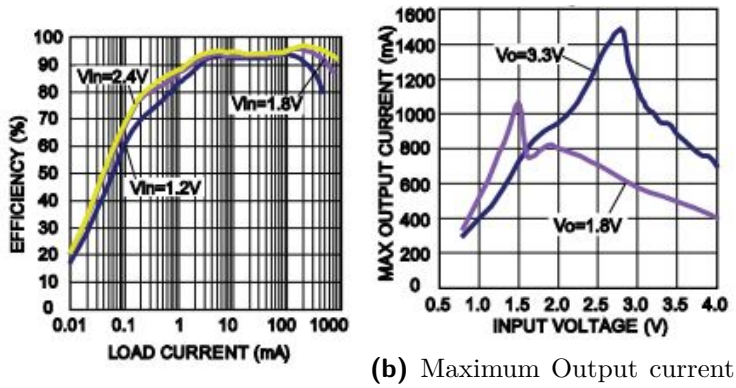

(a) Efficiency vs Load Current vs Input Voltage

(b) Maximum Output current

Figure 4.2: MP3414: Typical Characteristics. Reproduced from [23].

Results

The following output voltage, output current and efficiencies in Table 4.1 were obtained under heavy and light load with an input voltage 3.7V for both regulators.

Table 4.1: $V_{IN} = 3.7V$

Regulator	Load Condition	Output Voltage (V)	Output Current (mA)	Efficiency (%)
LTC3130-1	No Load	3.3	0	n/a
	Light Load	3.3	110	85
	Heavy Load	3.3	400	82
MP3414	No Load	3.6	0	n/a
	Light Load	3.6	50	86
	Heavy Load	3.6	650	88

The regulators were subjected to varying input voltages to analyze their performance, and the obtained results are presented in Tables D.1,D.2, and D.3.

Analysis

The LTC3130-1 showed efficient performance, especially under light-load conditions, consistent with expectations [16]. Operating at varying input voltage, the regulator maintained a stable 3.3V output across varying loads, with high efficiency even at heavy loads. These results align with the typical characteristics provided in Figure 4.1, confirming the effectiveness of Burst Mode in optimizing performance.

For the MP3414, despite using an unexpected version (MP3414 instead of MP3414A) and adjusting the design for a 3.6V output, the regulator demonstrated consistent behavior with expected characteristics. The output voltage, output current, and efficiency aligned well with the typical performance depicted in Figure 4.2. Tests at varying input voltages consistently showed stable output voltages and high efficiency, validating the regulators' robust performance across varying conditions.

4.2. Overcurrent Protection

Testing issue

During the experimental phase of testing the overcurrent protection circuit, an unforeseen challenge arose that prevented the successful execution of the test. The primary obstacle encountered was a short circuit between the bus voltage supplied to the overcurrent protection circuit and ground. Despite meticulous efforts, the exact location of this short circuit could not be identified.

Several factors might contribute to the difficulty in locating the short circuit:

- Multilayered PCB Design: The circuit is implemented on a multilayered PCB, the short circuit may occur between layers, making it difficult to detect visually
- Physical Damage: The short circuit might be a result of physical damage to the wiring or components, which may not be immediately visible during a visual inspection.

4.3. MPPT

A rheostat ranging from 0 to 30 ohms was used to characterize the performance of solar panels, with midday measurements capturing their response at peak solar intensity. Initial individual panel characterization was followed by assessing their combined performance in parallel, generating data points for I-V and P-V curves. Additionally, the impact of temperature on panel performance was studied by exposing them to 30 minutes of sunlight before collecting a new set of measurements, providing insights into the electrical characteristics affected by temperature variations induced by solar exposure. The resulting data and observations form a comprehensive basis for analyzing the MPPT algorithm's performance in conjunction with the characterized panels.

Expectations

For the I-V and P-V characteristics of the panel a similar trend as Figure 4.3 is expected.

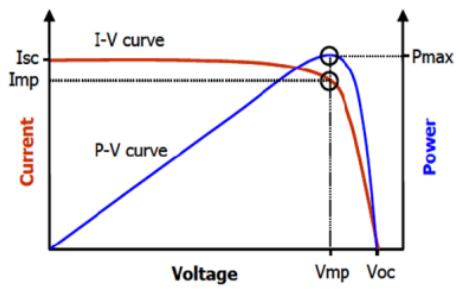

Figure 4.3: Typical I-V and P-V characteristics of a PV Cell. Reproduced from [6].

The MPPT algorithm is expected to track the MPP at around 1.4 V and 1.3 A of the panels and deliver approximately 1.8W of power.

Results

The detailed I-V and P-V curves of the panels are provided in Appendix D, Figures D.4 and D.5. A summary of the MPP results is presented in Table 4.2 below.

Test	Configuration	I_{MP} (A)	V_{MP} (V)	MPP (W)
1	Panel 1	0.68	1.39	0.9452
2	Panel 2	1.37	0.65	0.8905
3	Parallel Panels	1.4	1.32	1.848
4	Panel 1 (Higher Temperature)	1.36	0.66	0.8976
5	Panel 2 (Higher Temperature)	1.41	0.66	0.9306
6	Parallel Panels (Higher Temperature)	1.44	1.25	1.8

Table 4.2: Maximum Power Points for Different Tests

Following this, the panels were integrated into the MPPT system of the PocketQube, and the panel voltage and current were measured and recorded through current sensors and ADC channels of the microcontroller. Denoting the expected maximum power as $P_{\mathrm{MAX}} = 1.8\mathrm{W}$ and the actual power at each time step as P_{ACTUAL}, the percentage difference (Deviation) was calculated using the formula: $|\frac{P_{\mathrm{ACTUAL}}-P_{\mathrm{MAX}}}{P_{\mathrm{MAX}}}| \times 100$. Detailed results, including the % Deviation from the MPP, are presented in Appendix D, Table D.7 and Table D.8. A visual representation of the observed trend in power is illustrated in Figure 4.4.

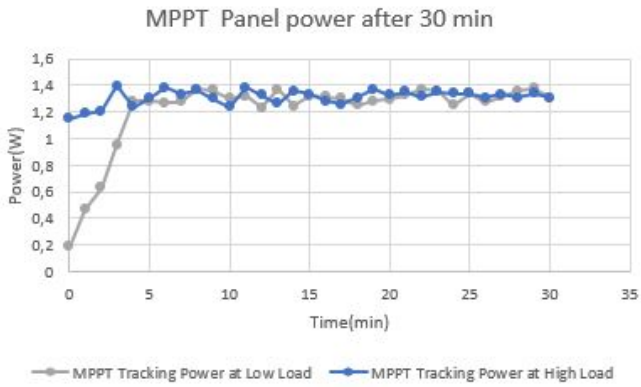

Figure 4.4: MPPT panel power after 30 min

Analysis

Analyzing the resultant data, it's clear that the algorithm is oscillating around a power output of approximately 1.3W after 4 min at high and low load instead of the expected 1.8W. The average accuracy over the 31 time steps is approximately 30%. This indicates

that the algorithm, on average, deviates from the expected maximum power by around 30%. In low light conditions the LTC3130-1 struggled to deliver the 5V output from the panels but had no problem delivering 5V at peak sunlight. The MPPC pin of the LTC3130-1 is very noise sensitive according to the datasheet and requires short trace lengths and widths. Further analysis, such as tuning the MPPT algorithm parameters or investigating environmental conditions, and IC limits may be necessary to improve the accuracy of the MPPT algorithm and bring the power output closer to the expected maximum.

4.4. BMS

The original design of the BMS was intended to be powered by a specific battery model, the specifications of which can be found in Table C.6, Appendix C, as specified in the initial project plan. However, due to unforeseen shipping delays with the ordered battery an alternative approach became necessary.

As a result, a generic off-the-shelf battery, the specifications of which can be found in Table C.5, Appendix C, was utilized to power the system.

Expectations

The designed battery charging circuit is expected to charge the battery in trickle charge mode which is 10% of the charge current until 2.8V, switch to CC mode and charge at the programmed 1A and then charge in CV mode after 4.1V as shown in Figure 4.5

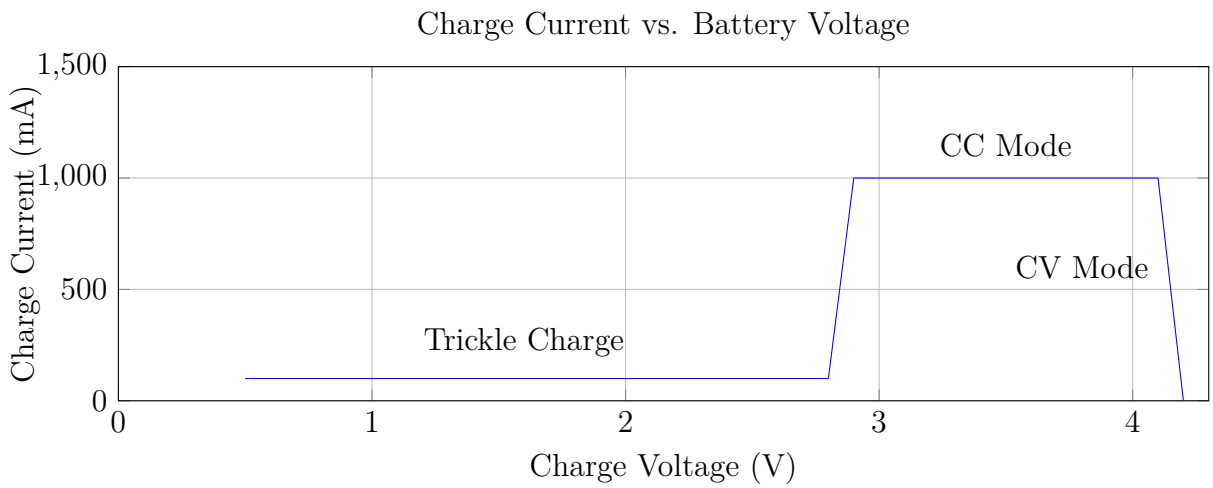

Figure 4.5: Charge Current vs. Charge Voltage expectation.

If the BMS functions through an external power supply, it is expected to function similarly through the MPPT system.

The Battery protection circuit is expected to switch off/ switch on the power to or from the battery according to the design parameters in Table C.7 in Appendix C.

Results

The battery was first charged on a bench power supply limited to 1A charge current and 4.2V charge voltage which match the design parameters of the BMS. The summarised results can be found in Table D.4 and Figure D.1

The battery was then safely discharged to about 50% SOC at 0.2C to prepare it for the testing and charged using the USB power supply feature on the LTC4066 and the programmed charge current of 1A of the LTC4066. The battery successfully charged through the USB power supply on the LTC4066 according to the characteristics in Table D.5 and Figure D.2 in Appendix D.

The MPPT, BMS and regulator system was now integrated together to test the functionality of the MPPT in charging the battery and supplying power to the bus. The battery was once again sucessfully charged through the MPPT system as power supply according to the characteristics in Table D.6 and Figure D.3 in Appendix D.

The combined results of all three charging methods can be found in Figure 4.6

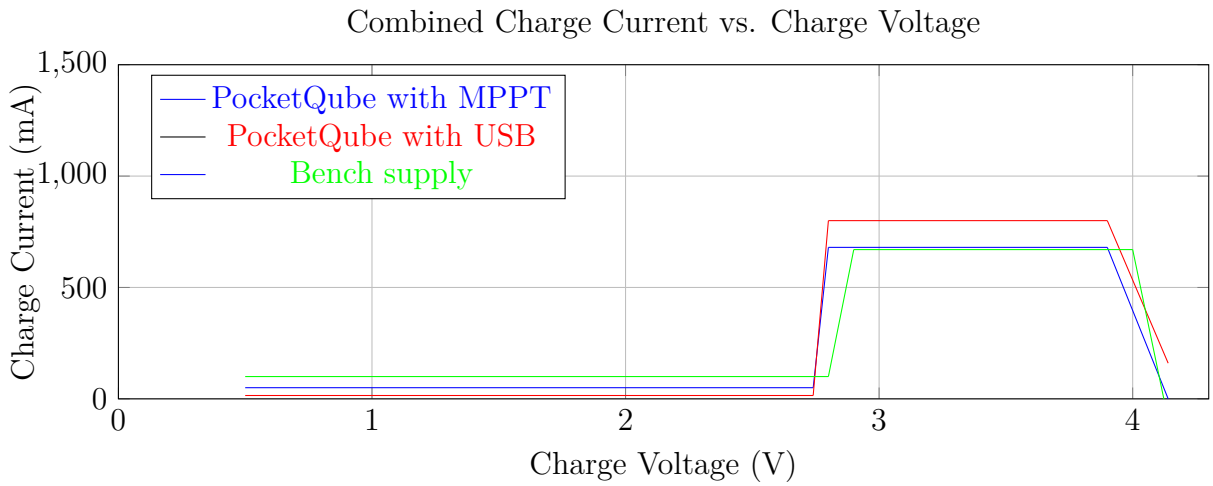

Figure 4.6: Combined Charge Current vs. Charge Voltage based on different charging methods.

The Battery protection circuit was implemented and tested on a seperate PCB due to space constraints on the designed PocketQube PCB. Different test conditions were applied and confirmed according to Table 4.3 below.

Table 4.3: Test Results for BQ29700 Design Parameters

Design Parameter	**Test Result**
Overvoltage Protection (OVP)	OVP triggered above 4.275V
Overvoltage Protection (OVP) release voltage	OVP released below 4.175 V
Undervoltage Protection (UVP)	UVP triggered below 2.8V
Undervoltage Protection (UVP) release voltage	UVP released above 2.9V
Charge Overcurrent detection (OCC) voltage	OCC triggered
Discharge Overcurrent Detection (OCD) voltage	OCD triggered
Load Short Circuit Detection (SCC) voltage	SCC triggered
Load Short Circuit release voltage	SCC released

Analysis

The combined charge current vs charge voltage plots for three charging methods—PocketQube with MPPT, PocketQube with USB, and Bench supply—reveal distinct charging characteristics similar to what was expected. In all cases, the systems exhibit Trickle Charge, Constant Current (CC) Mode, and Constant Voltage (CV) Mode. Notably, the PocketQube with MPPT and USB both show a linear increase in charge current during CC Mode, peaking around 680 mA and 800 mA, respectively, before decreasing during CV Mode. Similarly, the Bench supply peaks at approximately 670 mA during CC Mode. The IC might not charge according to the programmed 1 A charge current for various reasons. Potential factors include the solar panels and the USB used during testing not being able to provide enough power to power the load connected on the subsystem side and charge the battery at the same time. When the solar panel input was disconnected the ideal diode function of the LTC4066 worked in switching the bus power to the battery instead of the panel.

Chapter 5: Conclusion

In this project, the aim was to design and implement a solar-powered PocketQube satellite power subsystem, consisting of a MPPT system, a BMS, and power regulators and distribution. The goal was to achieve efficient solar power harvesting, energy storage, and distribution for the satellite's subsystems all within the physical constraints of the PocketQube.

5.1. MPPT System

The MPPT system was designed to optimize solar panel power output by tracking the Maximum Power Point (MPP) in varying lighting conditions. A Perturb and Observe (P&O) MPPT algorithm was implemented. The system successfully tracked the MPP, adjusting the operating point of the solar panels to maximize power generation. However, the observed power output was below the expected maximum in both high and low light conditions, with an average deviation of approximately 30%. Further optimization of the MPPT algorithm, considering system constraints, environmental factors, and IC limitations, is recommended.

5.2. Battery Management System (BMS)

The BMS was designed to charge and protect the battery, ensuring optimal performance and longevity. The LTC4066 was selected as the battery charger, offering USB/Solar charging and a high charge current capability. The BQ29700 was chosen for battery protection, providing features such as overvoltage, undervoltage, and overcurrent protection. The BMS successfully charged the battery through multiple methods: a bench power supply, USB power from the LTC4066, and solar power through the MPPT system. The BQ29700 protection features were tested and confirmed to operate according to the design parameters.

5.3. Regulators

The power distribution system included regulators (LTC3130-1 and MP3414) to regulate the voltage for subsystems. The regulators demonstrated efficient performance of average 85%, maintaining stable output voltages under varying loads and input conditions.

5.4. Challenges and Recommendations

The project faced challenges such as unexpected component delays, which led to modifications in the design and testing plan. The inductor footprints were wrong which led to modification of PCB through use of wires to be able to connect the inductors. The 90° header connection was 4mm too low and thus not according to specifications. The MPPT system showed deviations from the expected maximum power output, suggesting the need for further tuning of the MPPT algorithm and consideration of environmental factors. The Overcurrent protection circuit contained an unexpected short circuit in the main power supply bus that could not be found.

Recommendations for future work include:

- Further optimization of the MPPT algorithm to enhance accuracy and adaptability to varying conditions.
- Comprehensive testing under simulated space conditions to validate subsystem performance in a space environment.
- Investigation into power losses within the system to identify areas for improvement.
- Exploration of alternative MPPT algorithms or hybrid approaches to enhance overall efficiency.
- Integration of temperature and environmental sensors to account for external factors affecting system performance.
- Consideration of the impact of load variations and transient conditions on the power subsystem.
- Investigation into the power budget of the PocketQube, allowing certain subsystems to be powered through the EPS according to a schedule.
- Re-evaluation of the PCB design to fix schematic and design bugs.

Despite the challenges, the project successfully demonstrated the functionality of the designed power subsystem components. Further refinement and testing under space-simulated conditions will contribute to the development of a robust and efficient power subsystem for PocketQube satellites.

Bibliography

[1] S. Radu, M. Uludag, S. Speretta, J. Bouwmeester, A. Menicucci, A. Cervone, A. Dunn, T. Walkinshaw, P. K. D. Cas, C. Cappelleti, and F. Graziani, "PocketQube Mechanical Interface Standard." DataverseNL, 2018. [Online]. Available: https://doi.org/10.34894/FOBWZU

[2] D. Slabber., *Pocketcube Mechanical Interface*, 2023.

[3] S. Speretta, T. Soriano, J. Bouwmeester, J. Carvajal-Godínez, A. Menicucci, T. Watts, P. Sundaramoorthy, J. Guo, and E. Gill, "Cubesats to pocketqubes: Opportunities and challenges," 09 2016.

[4] S. Li and H. Zheng, "Energy extraction characteristic study of solar photovoltaic cells and modules," in *2011 IEEE Power and Energy Society General Meeting*, 2011, pp. 1–7.

[5] Lesics. How do solar cells work? Youtube. [Online]. Available: https://youtu.be/L_q6LRgKpTw?si=BPtxF5MX65lf8sDi

[6] P. Singh, A. Balyan, Gangadhara, and S. Prabhu M, "P-v and i-v characteristics of solar cell," *Design Engineering (Toronto)*, 06 2021.

[7] A. Sheikholeslami, "Buck and boost converters [circuit intuitions]," *IEEE Solid-State Circuits Magazine*, vol. 13, no. 4, pp. 12–14, 2021.

[8] S. Motahhir, A. El Hammoumi, and A. El Ghzizal, "The most used mppt algorithms: Review and the suitable low-cost embedded board for each algorithm," *Journal of cleaner production*, vol. 246, p. 118983, 2020.

[9] M. Yaqoob, H. Abubakr, J. M. Alcala, A. Lashab, J. M. Guerrero, and J. C. Vasquez, "A comparative study of mppts for nano-satellite microgrid applications under spinning flight scenarios," in *IECON 2022 – 48th Annual Conference of the IEEE Industrial Electronics Society*, 2022, pp. 1–6.

[10] B. Gmati, A. Hmidet, O. Hasnaoui, and R. Dhifaoui, "Exprimental study of mppt algorithms for pv solar water pumping applications," 03 2014.

[11] D. Beriber and A. Talha, "Mppt techniques for pv systems," in *4th International Conference on Power Engineering, Energy and Electrical Drives*, 2013, pp. 1437–1442.

[12] E. Schwanbeck and P. Dalton, "International space station lithium-ion batteries for primary electric power system," in *2019 European Space Power Conference (ESPC)*, 2019, pp. 1–1.

[13] D. Deng, "Li-ion batteries: basics, progress, and challenges," *Energy Science Engineering*, vol. 3, 09 2015.

[14] B. Arabsalmanabadi, N. Tashakor, A. Javadi, and K. Al-Haddad, "Charging techniques in lithium-ion battery charger: Review and new solution," in *IECON 2018 - 44th Annual Conference of the IEEE Industrial Electronics Society*, 2018, pp. 5731–5738.

[15] "Charging method — charge control ics — electronics basics — rohm," https://www.rohm.com/electronics-basics/battery-charge/charging-method, 2023, accessed: 2023-10-22.

[16] *25V, 600mA Buck-Boost DC/DC Converter with 1.6Quiescent Current*, Linear Technology, 2016, rev. D. [Online]. Available: https://www.analog.com/media/en/technical-documentation/data-sheets/3130f.pdf

[17] *USB Power Controller and Li-Ion Linear Charger with Low Loss Ideal Diode*, Linear Technology, 2005, rev. D. [Online]. Available: https://www.analog.com/media/en/technical-documentation/data-sheets/4066fc.pdf

[18] *BQ297xx Cost-Effective Voltage and Current Protection Integrated Circuit for Single Cell Li-Ion and Li-Polymer Batteries*, Texas Instruments, 2014, rev. D. [Online]. Available: https://www.ti.com/lit/ds/symlink/bq2970.pdf?ts=1698947583223&ref_url=https%253A%252F%252Fwww.ti.com%252Fproduct%252FBQ2970

[19] *3A, 1MHz, 22A Iq, 5.5V Synchronous Step-Up Converter with Output Disconnect*, MPS, 2014, rev. D. [Online]. Available: https://pdf1.alldatasheet.com/datasheet-pdf/view/1036103/MPS/MP3414A.html

[20] *TPS256x Dual Channel Precision Adjustable Current-limited Power Switches*, Texas Instruments, 2020, rev. D. [Online]. Available: https://www.ti.com/lit/ds/symlink/tps2561.pdf?ts=1698164101040

[21] *INA1x8 High-Side Measurement Current Shunt Monitor*, Texas Instruments, 2017, rev. D. [Online]. Available: https://www.ti.com/product/INA138

[22] M. Oredsson, "Electrical power system for the cubestar nanosatellite," 2010. [Online]. Available: https://api.semanticscholar.org/CorpusID:63181656

[23] *1.8A,1MHz, Synchronous, Step-up Converter with Output Disconnect*, MPS, 2018, rev. D. [Online]. Available: https://www.monolithicpower.com/en/documentview/productdocument/index/version/2/document_type/Datasheet/lang/en/sku/MP3414/document_id/1153/

[24] *8-bit AVR Microcontroller with 32K Bytes In-System Programmable Flash*, Atmel, 201, rev. D. [Online]. Available: https://ww1.microchip.com/downloads/en/DeviceDoc/Atmel-7810-Automotive-Microcontrollers-ATmega328P_Datasheet.pdf

[25] *16340 Lipo Battery 3.7V 700mAh Li-ion (CR123A)*, MicroRobotics, 2014, rev. D. [Online]. Available: https://www.robotics.org.za/16340?search=1634

[26] *RS PRO, 3.7V, 18650, Lithium-Ion Rechargeable Battery, 2.6Ah*, RS Pro, 2014, rev. D. [Online]. Available: https://docs.rs-online.com/9c01/A700000008874176.pdf

Appendix A

Project Planning Schedule

Table A.1: Project Schedule

Task	Duration	Start Date	End Date
Literature Review	15 days	Mon 23/07/31	Fri 23/08/18
MPPT	5 days	Mon 23/07/31	Fri 23/08/04
Battery Management	5 days	Mon 23/08/07	Fri 23/08/11
Power Management	5 days	Mon 23/08/14	Fri 23/08/18
Literature Review Complete	0 days	Fri 23/08/18	Fri 23/08/18
Design	29 days	Mon 23/08/21	Thu 23/09/28
Selection and ordering of components	2 days	Mon 23/08/21	Tue 23/08/22
MPPT design	7 days	Wed 23/08/23	Thu 23/08/31
Battery Management Design	10 days	Fri 23/09/01	Thu 23/09/14
Power Management Design	10 days	Fri 23/09/15	Thu 23/09/28
Design Phase complete	0 days	Thu 23/09/28	Thu 23/09/28
Manufacturing and Testing	24 days	Fri 23/09/29	Wed 23/11/01
Prepare for Manufacturing	2 days	Fri 23/09/29	Mon 23/10/02
Manufacturing	12 days	Tue 23/10/03	Wed 23/10/18
Testing	9 days	Thu 23/10/19	Tue 23/10/31
Report Writing	65 days	Tue 23/08/08	Mon 23/11/06
Draft Hand-In to supervisor	1 day	Wed 23/10/25	Wed 23/10/25

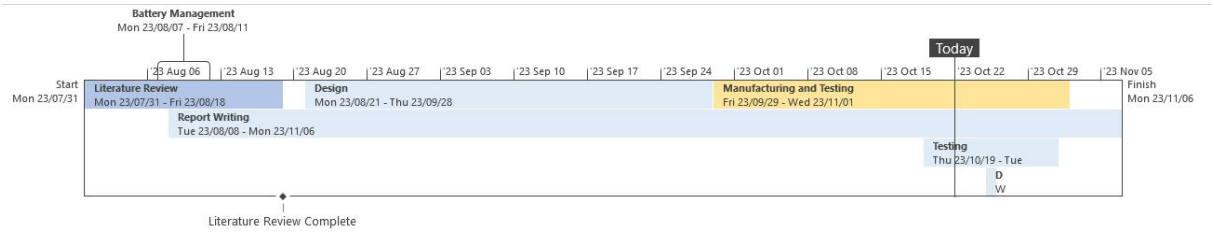

Figure A.1: Project Gantt Chart

Appendix B

Outcomes Compliance

Outcome	Motivation	Sections
GA 1: Problem Solving	The project starts by asking research questions describing the problem faced and setting goals to be able to answer each of them. Research is first done to find the best fit methods allowing us to solve these problems. The methods are then realized in design and implementation to allow testing. After testing, the goals are evaluated by what degree it has been achieved and if further improvement is required. Some problems were faced during the testing phase with regards to PCB errors, incorrect components, incorrect outputs, which required debugging and workarounds to be able to continue.	1.2, 2.1, 2.3, 2.4, 2.5, 3.1, 3.2, 3.3, 3.4, 3.5, 3.6, 4.2, 4.3, 4.4
GA 2: Application of scientific and engineering knowledge	The project used newly obtained knowledge in related fields such as the space and solar industry regarding solar energy harvesting, battery management and power regulation and distribution as well as background knowledge in calculus, electronics, programming and designing to, design the EPS system in both hardware and software.	2.1, 2.2, 2.3, 2.4, 2.5, 3.1, 3.2, 3.3, 3.4, 3.5, 3.6
GA 3: Engineering Design	The project used a systematic design approach to implement an EPS system. The proposed methodology includes conducting design research, initial component selection, system design, prototyping, rigorous testing and refinement.	3.2, 3.3, 3.4, 3.5, 3.6, 4.1, 4.2, 4.4, 4.3, **??**

GA 4: Investigations, experiments and data analysis	Experimental designs were set up before each component was tested. Engineering tools were utilized to investigate functionality of the system according to experimental design and expectations. Data was recorded and graphed on Excel to be analyzed and compared to expectations. All differences in results and expectations were thoroughly investigated in order to provide solutions.	3.4.3, 3.2.3, 3.3.3, 3.5.3, 4.1, 4.2, 4.4, 4.3, **??**, D
GA 5: Engineering methods, skills and tools, including Information Technology	KiCad was used to realize an EPS system in hardware. Software tools such as Python, Arduino IDE, and Excel were used for data analysis, graphing and programming. Engineering tools used in the experiment phase include Multimeters, soldering iron, oscilloscope, bench power supply, wiring, breadboarding, Function generator to allow for extensive testing of the system. Microsoft Project was used to set up a project plan and make changes to the plan	3.2, 3.3, 3.4, 3.5, 3.6, 4.1, 4.2, 4.4, 4.3, **??**, A, E, F, D
GA 6: Professional and technical communication	The technical literature and design are communicated through professional writing and crafted visuals. The final report adheres to academic standards in terms of writing, formatting, styling, and language use, and it was exclusively composed using LaTeX. The project encompasses a comprehensive written report and an articulate oral presentation. Together, these components showcase competence in effective communication, demonstrating proficiency both in written expression and oral presentation skills.	All sections
GA 8: Individual Work	All aspects of the project were done individually and only under supervision	All sections

GA 9: Independent Learning Ability	PCB designing was self-taught through research and tutorials. The concept of PocketQubes was new and had to be researched to get a full understanding of what is being built and the standards behind it. Switched regulators (Buck and Boost), although covered in a separate module in the energy stream (Electronics 414, week 4, lecture 11) of the undergraduate course, were not covered in the robotics stream and thus had to be covered in literature. All other aspects of the literature review were completely newly obtained knowledge obtained through research papers and the internet, not covered in the undergraduate course. Further knowledge and experience on component selection and using datasheets are developed for the design of the system. KiCad introduced a new learning curve on schematic and PCB design to allow implementation of the system. Learning how to flash code onto a microcontroller (ATMEGA328p) through the use of SPI on the Arduino NANO.	2.1, 2.2, 2.3, 2.4, 2.5, 3.2, 3.3, 3.4, 3.5, 3.6

Appendix C

Components Characteristics

C.1. LTC3130-1

Table C.1: Desired Characteristics of LTC3130-1 for MPPT. Adapted from [16].

Characteristic		**Description**
Input Voltage Range	2.4 -25V	Wide input voltage range to accommodate varying solar cell outputs.
Output Voltage Range	1 - 35V	Wide output voltage range to accomodate battery charger
Efficiency	up to 95%	High efficiency for effective power conversion.
MPPT	Programmable MPPC pin	Ability to perform MPPT to ensure maximum power extraction from solar cells.
Analog Voltage Input	-0.3 - 6V	Capability to accept an analog voltage signal from the MPPT algorithm.
Current Limiting	850mA/450mA programmable	Feature to limit input current to protect the LTC3130 and the EPS.
Temperature Range	$-40 - 125°C$	Operating temperature range suitable for space applications.
Size	3mm	Compact size to fit within the picosatellite's EPS subsystem.

Click 3.2 to return to MPPT design.

C.2. ATmega328P

Table C.2: Desired Characteristics of ATmega328P 8-bit AVR Microcontroller. Adapted from [24].

Feature		**Description**
Architecture	Advanced RISC	High-performance, low-power AVR® 8-bit microcontroller with advanced RISC architecture.
Instructions	131 powerful instructions	Most single clock cycle execution for efficient operation.
Registers	32, 8 general-purpose registers	Ample general-purpose working registers for versatile application development.
Clock Speed	Up to 16 MIPS at 16MHz	Fully static operation with a high throughput of up to 16 MIPS at 16MHz.
Memory	32K bytes Flash, 1K bytes EEPROM, 2K bytes SRAM	High-endurance non-volatile memory segments for program and data storage.
Peripheral Features	Timers, PWM channels, ADC, USART, SPI, I2C, RTC, Analog Comparator	Rich set of peripheral features for diverse applications.
Watchdog Timer	Programmable watchdog timer	Programmable watchdog timer with a separate on-chip oscillator.
Power Management	Six sleep modes	Six sleep modes for efficient power consumption: Idle, ADC noise reduction, power-save, power-down, standby, and extended standby.
Operating Voltage	2.7V to 5.5V	Wide operating voltage range for flexibility.
Temperature Range	-40°C to +125°C	Suitable for automotive temperature applications.
Speed Grades	0 to 8MHz, 0 to 16MHz	Multiple speed grades to meet different performance requirements.
Power Consumption	Active mode: 1.5mA at 3V - 4MHz, Power-down mode: 1µA at 3V	Low power consumption in both active and power-down modes.

Click 3.2.2 to return to MPPT software.

C.3. MP3414A

Table C.3: Desired Characteristics of MP3414A. Adapted from [19].

Characteristic		**Description**
Input Voltage Range	1.8 - 5.5V	Suitable input voltage range for various power sources.
Output Voltage Range	1.8 - 5.5V	Adjustable output voltage to meet different load requirements.
Peak Switching Current	$> 3A$	High peak switching current capability for handling varying
Efficiency	Up to 97%	High efficiency for effective power conversion.
Start-Up Voltage	1.8V	Ability to start up from a low input voltage for enhanced flexibility.
Output Short-Circuit Protection	Yes	Integrated protection against output short circuits for increased reliability.
Quiescent Current	22uA	Low quiescent current for power efficiency during standby.
Switching Frequency	1MHz	Fixed switching frequency allowing the use of small external components.
Package	TSOT23-8	Available in a small TSOT23-8 package for compact designs such as picosatellite's EPS.

Click 3.4 to return to regulators design.

C.4. LTC4066

Table C.4: Desired Characteristics of LTC4066 for Battery Charging and Power Management. Adapted from [17].

Characteristic		**Description**
Maximum Charge Current	1.5A	Allows for efficient charging of Li-Ion batteries.
Input Supply Voltage	4.35 - 5.5V	Operating range for seamless transition between input power sources (Li-Ion battery, USB, and 5V wall adapter).
Input Voltage for Battery	4.3V	Input voltage for the Li-Ion battery.
Power Source Transition	Seamless Transition	Smooth transition between Li-Ion battery, USB, and 5V wall adapter as power sources.
Ideal Diode Path	Low Loss ($50m\Omega$)	Provides a low-loss ideal diode path from the battery to the output.
Programmable Charge Current Detection	Yes	Enables programmable charge current detection (CHRG).
Analog Gas Gauge Function	Yes	Provides an analog gas gauge function for battery monitoring.
Constant-Current/Constant-Voltage Operation	Yes	Maximizes charging rate with thermal feedback to prevent overheating.
Termination Timer	Yes	Adapts to actual charge current, optimizing charging efficiency.
Charge Voltage	4.2V (4.1V for LTC4066-1)	Preset charge voltage with high accuracy.
Package	24-Lead 4mm × 4mm QFN (0.75mm profile)	Compact package suitable for compact designs.

Click 3.3 to return to BMS design.

C.5. Li-ion Battery

Table C.5: Test Battery Specifications. Adapted from [25]

Parameter	Value	Unit
Capacity	700	mAh
Nominal Voltage	3.7	V
Chemistry	Li-ion	-
Charging Voltage	4.2	V
Standard Charge Current	140	mA
Quick Charge Current	700	mA
Dimensions	35.3 x 16.5	mm
Energy Density	2.58	wH

Table C.6: Ordered Battery Specifications. Adapted from [26]

Parameter	Value	Unit
Capacity	2600	mAh
Nominal Voltage	3.7	V
Chemistry	Li-ion	-
Charging Voltage	4.2	V
Standard Charge Current	480	mA
Quick Charge Current	2400	mA
Dimensions	70 x 18.9	mm
Overcharge Detection Voltage	4.280 ± 0.025	V
Overcharge Detection Delay Time	0.92-1.4	s
Over Discharge Detection Voltage	2.800 ± 0.050	V
Over Discharge Detection Delay Time	115-173	ms
Discharge Over Current Detection	5.0-9.0	A
Over Current Detection Delay Time	7.2-11.0	ms
Short Circuit Detection Delay Time	220-360	μs
Current Consumption In Normal	3	μA (Type), 6.0 μA (Max)

C.6. BQ29700

Table C.7: Design Parameters for BQ29700. Reproduced from [18].

DESIGN PARAMETER	EXAMPLE VALUE at TA = 25°C
Input voltage range	4.5 V to 7 V
Maximum operating discharge current	7 A
Maximum Charge Current for battery pack	4.5 A
Overvoltage Protection (OVP)	4.275 V
Overvoltage detection delay timer	1.2 s
Overvoltage Protection (OVP) release voltage	4.175 V
Undervoltage Protection (UVP)	2.8 V
Undervoltage detection delay timer Undervoltage Protection (UVP) release voltage	150 ms 2.9 V
Charge Overcurrent detection (OCC) voltage	–70 mV
Charge Overcurrent Detection (OCC) delay timer	9 ms
Discharge Overcurrent Detection (OCD) voltage	100 mV
Discharge Overcurrent Detection (OCD) delay timer	18 ms
Load Short Circuit Detection (SCC) voltage, BAT to –V threshold	500 mV
Load Short Circuit Detection (SCC) delay timer	250 µs
Load Short Circuit release voltage, BAT to –V Threshold	1 V

Click 3.3.2 to return to BMS design.

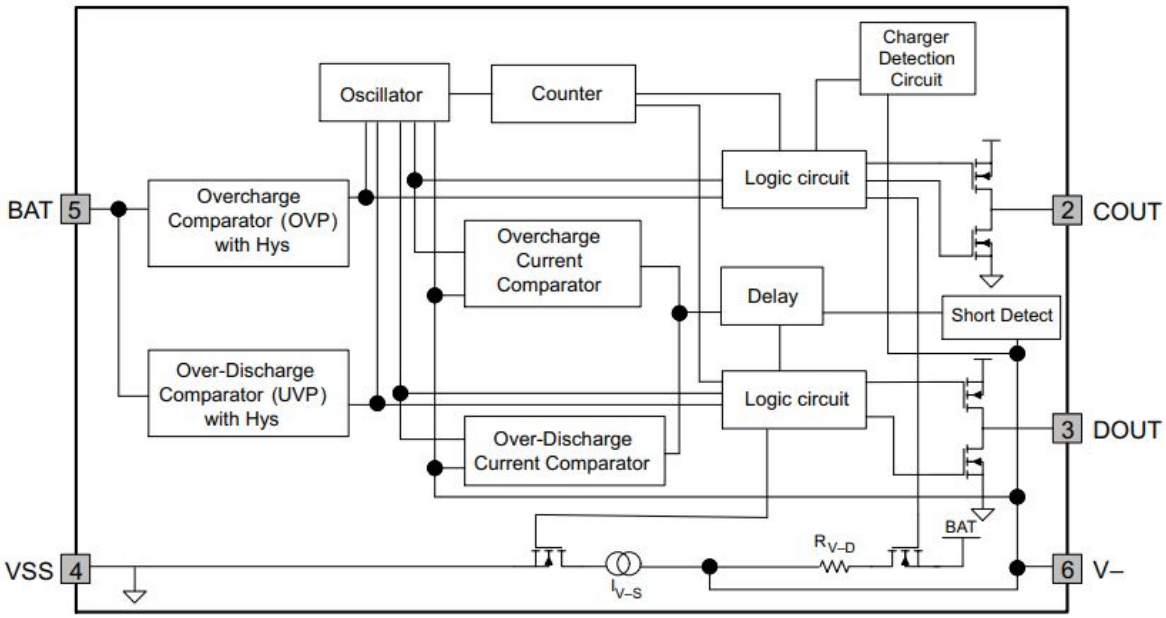

Figure C.1: Functional Block Diagram for BQ29700. Reproduced from [18].

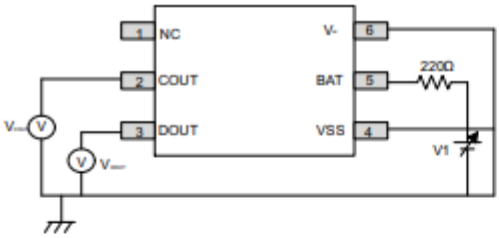

Figure 8-3. Test Circuit 1

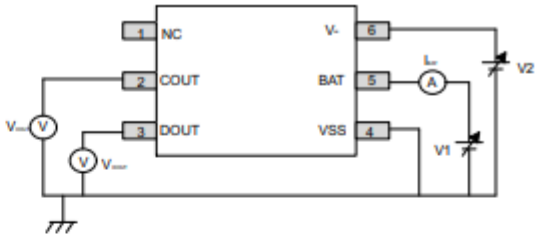

Figure 8-4. Test Circuit 2

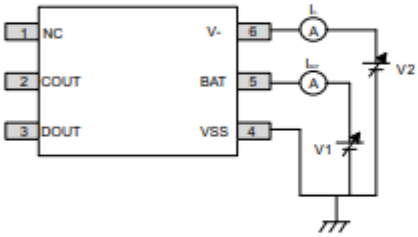

Figure 8-5. Test Circuit 3

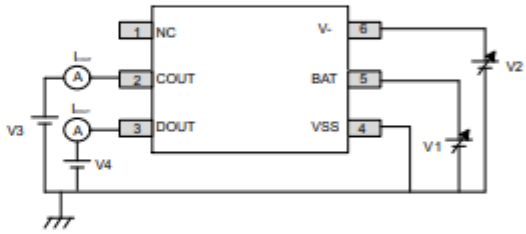

Figure 8-6. Test Circuit 4

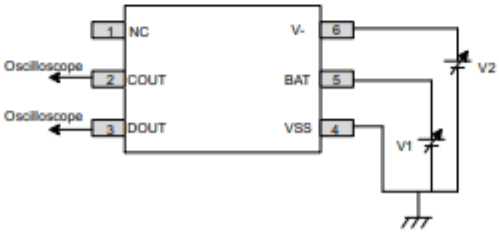

Figure 8-7. Test Circuit 5

Figure C.2: Test Circuits for BQ29700. Reproduced from [18].

Appendix D

Results Graphs and Tables

Table D.1: $V_{IN} = 3V$

Regulator	Load Condition	Output Voltage (V)	Output Current (mA)	Efficiency (%)
LTC3130-1	No Load	3.3	0	n/a
	Light Load	3.3	90	88
	Heavy Load	3.3	350	78
MP3414	No Load	3.6	0	n/a
	Light Load	3.6	45	88
	Heavy Load	3.6	620	90

Table D.2: $V_{IN} = 3.3V$

Regulator	Load Condition	Output Voltage (V)	Output Current (mA)	Efficiency (%)
LTC3130-1	No Load	3.3	0	n/a
	Light Load	3.3	40	88
	Heavy Load	3.3	350	88
MP3414	No Load	3.6	0	n/a
	Light Load	3.6	60	85
	Heavy Load	3.6	700	86

Table D.3: $V_{IN} = 5V$

Regulator	Load Condition	Output Voltage (V)	Output Current (mA)	Efficiency (%)
LTC3130-1	No Load	3.3	0	n/a
	Light Load	3.3	80	88
	Heavy Load	3.3	450	74
MP3414	No Load	3.6	0	n/a
	Light Load	3.6	40	80
	Heavy Load	3.6	590	82

Table D.4: Li-ion Battery Parameters During Charging on Bench Power Supply

Charging Voltage (V)	Charge Current (mA)
2.7	100
2.82	100
3.04	670
3.96	670
3.98	670
4.0	670
4.1	670
4.1	670
4.1	450
4.1	190
4.1	80
4.1	70
4.1	50

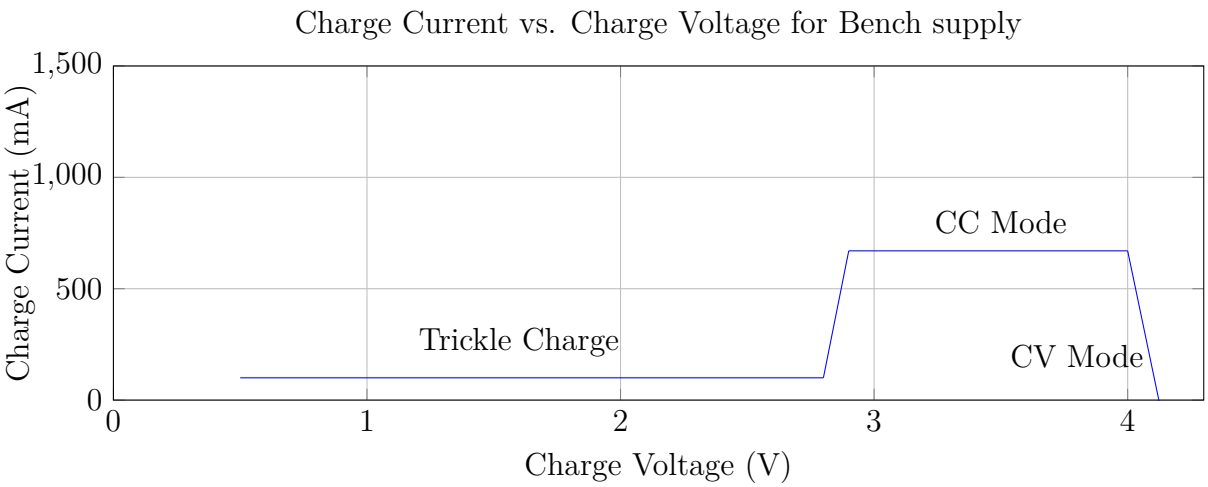

Figure D.1: Charge Current vs. Charge Voltage based on Table D.4.

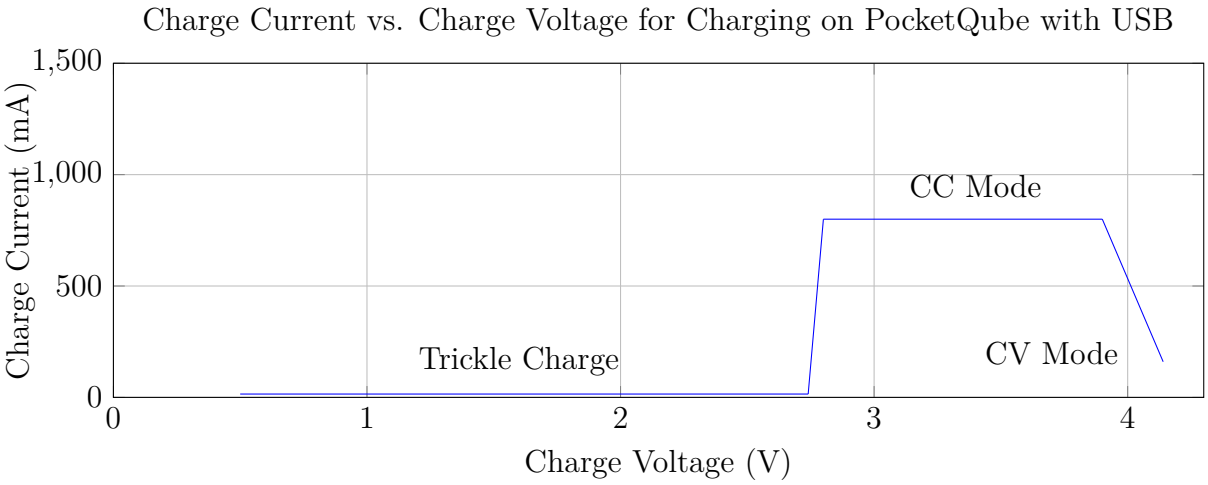

Figure D.2: Charge Current vs. Charge Voltage based on Table D.5.

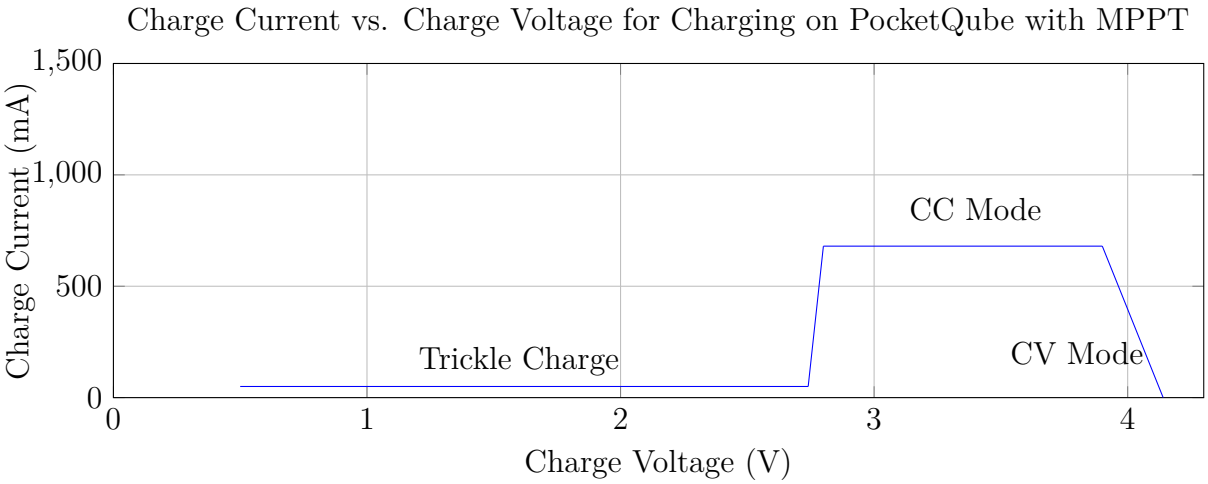

Figure D.3: Charge Current vs. Charge Voltage based on Table D.6.

Table D.5: Li-ion Battery Parameters During Charging on PocketQube with USB

Charge voltage(V)	Charge Current (mA)
2.6 1	15
2.62	15
2.64	15
2.66	10
2.67	10
2.69	10
2.70	10
2.72	10
2.74	10
2.76	800
2.80	800
2.86	800
2.96	800
3.10	800
3.23	800
3.30	800
3.45	800
3.56	800
3.66	800
3.78	800
3.90	800
4.07	500
4.11	320
4.13	150
4.14	60
4.14	20

Table D.6: Li-ion Battery Parameters During Charging on PocketQube with MPPT

Charge voltage(V)	Charge Current (mA)
2.64	50
2.67	50
2.69	50
2.70	50
2.72	50
2.74	50
2.75	50
2.77	50
2.79	50
2.80	680
2.84	680
2.90	680
3.06	680
3.20	680
3.33	680
3.41	680
3.55	680
3.60	680
3.69	680
3.80	680
3.93	680
4.04	680
4.11	150
4.13	70
4.13	60
4.14	20

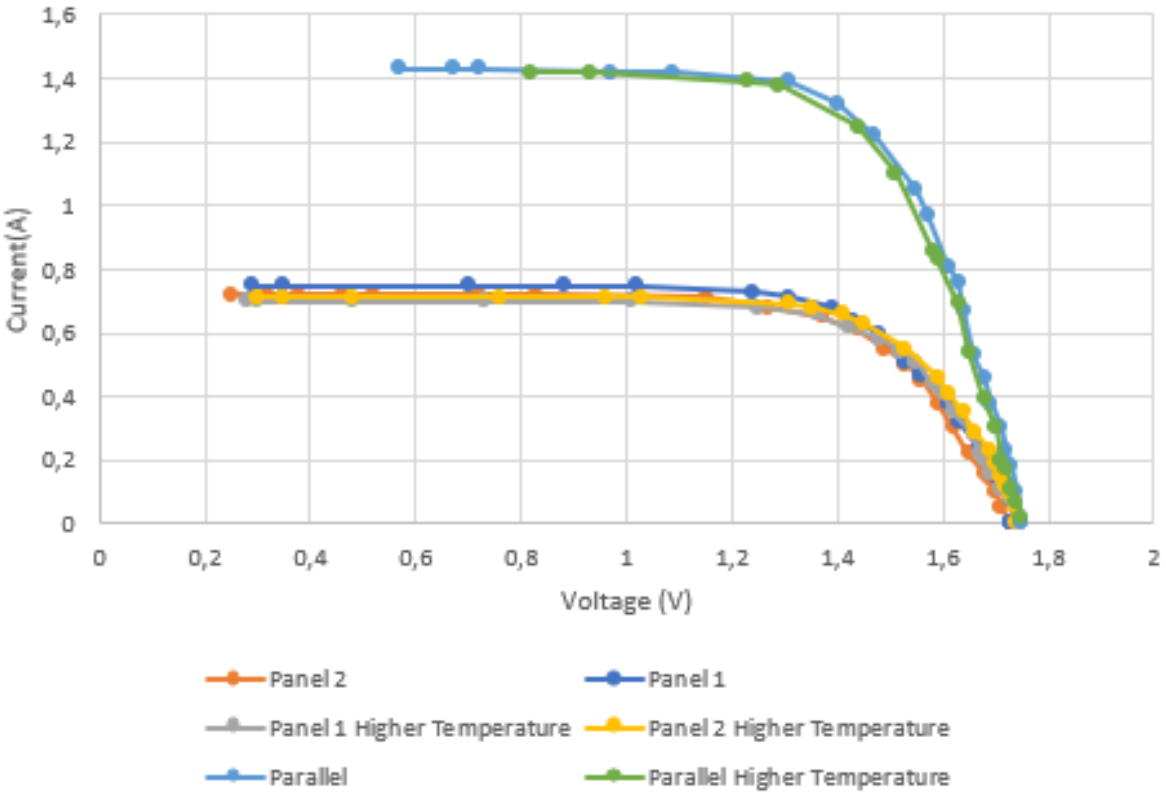

Figure D.4: I-V Characteristics of Panels

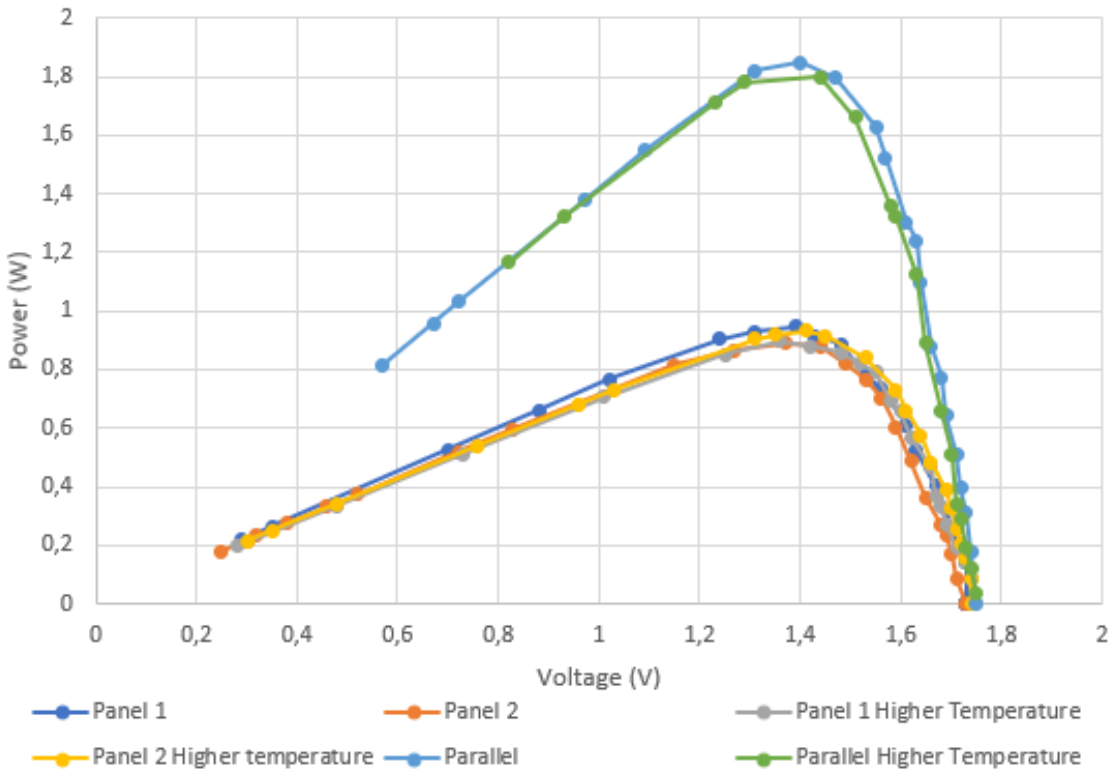

Figure D.5: P-V Characteristics of Panels

Table D.7: MPPT Algorithm Results and Accuracy at high load

Min	Voltage (V)	Current (I)	Power (W)	Deviation (%)
0	0.9568	1.2008	1.14892544	36.17
1	0.9879	1.2	1.18548	34.14
2	1.1258	1.07213	1.207003954	32.94
3	1.33565	1.04354346	1.393808822	22.57
4	1.1936	1.0356767	1.236183709	31.32
5	1.24128	1.045664	1.29796181	27.89
6	1.3223	1.044444	1.381068301	23.27
7	1.2479	1.06992	1.335153168	25.82
8	1.33214	1.023234	1.363090941	24.27
9	1.2433	1.047856	1.302799365	27.62
10	1.2122	1.02001	1.236456122	31.31
11	1.344	1.029285714	1.38336	23.15
12	1.2887	1.027738095	1.324446083	26.42
13	1.22767	1.026190476	1.259823262	30.01
14	1.3245	1.024642857	1.357139464	24.60
15	1.30076	1.023095238	1.330801362	26.07
16	1.2557	1.021547619	1.282757345	28.74
17	1.23444	1.02	1.2591288	30.05
18	1.28395	1.018452381	1.307641935	27.35
19	1.34664	1.016904762	1.369404629	23.92
20	1.3053	1.015357143	1.325345679	26.37
21	1.33553	1.013809524	1.353973033	24.78
22	1.2995	1.012261905	1.315434345	26.92
23	1.3365	1.010714286	1.350819643	24.95
24	1.3244	1.009166667	1.336540333	25.75
25	1.32954	1.007619048	1.339669829	25.57
26	1.2986	1.006071429	1.306484357	27.42
27	1.32378	1.00452381	1.329768529	26.12
28	1.3002	1.00297619	1.304069643	27.55
29	1.33564	1.001428571	1.337548057	25.69
30	1.30503	0.999880952	1.304874639	27.51

Table D.8: MPPT Algorithm Results and Accuracy at low load

Min	Voltage (V)	Current (I)	Power (W)	Deviation (%)
0	0.2134	0.87555	0.18684237	89.62
1	0.4523	1.023342	0.462857587	74.29
2	0.5886	1.07123	0.630525978	64.97
3	0.8233	1.155453	0.951284455	47.15
4	1.1009	1.16122	1.278387098	28.98
5	1.2407	1.034908174	1.284010571	28.67
6	1.2479	1.019038522	1.271658171	29.35
7	1.281230809	1.023973746	1.277816838	29.01
8	1.328015292	1.033871826	1.372997596	23.72
9	1.340454372	1.015729463	1.361538999	24.36
10	1.276364139	1.020902309	1.303043096	27.61
11	1.277778424	1.030775866	1.317103161	26.83
12	1.214713098	1.014768153	1.232652166	31.52
13	1.347935668	1.014405757	1.367353701	24.04
14	1.212533809	1.026072834	1.244148002	30.88
15	1.285905271	1.024088103	1.316880289	26.84
16	1.28547652	1.02153502	1.313159282	27.05
17	1.276580791	1.016659756	1.297848316	27.90
18	1.213598959	1.027748771	1.247274838	30.71
19	1.251727781	1.026201468	1.284524886	28.64
20	1.259485258	1.027867106	1.294583467	28.08
21	1.286298103	1.030044567	1.324944372	26.39
22	1.325431036	1.033932574	1.370406323	23.87
23	1.324586716	1.025946411	1.358954988	24.50
24	1.229250552	1.019098792	1.252727753	30.40
25	1.30035129	1.030871042	1.340494489	25.53
26	1.247474448	1.021163519	1.273875397	29.23
27	1.277089824	1.030158682	1.315605171	26.91
28	1.32853687	1.022790746	1.358815216	24.51
29	1.333618614	1.031900668	1.376161939	23.55
30	1.285634546	1.016221041	1.306488876	27.42

Appendix E

Schematics

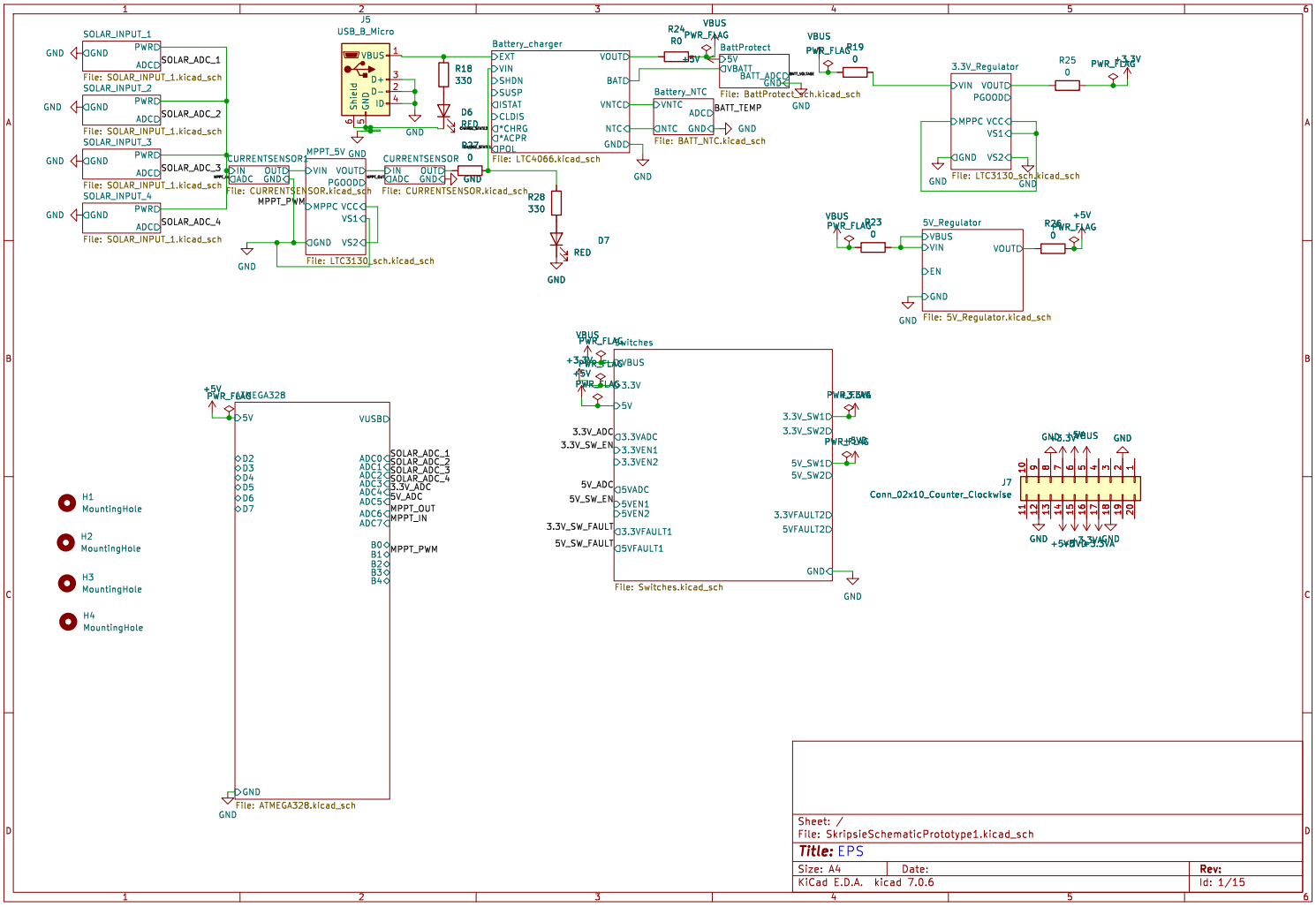
SOLAR_INPUT_1
SOLAR_ADC_1
File: SOLAR_INPUT_1.kicad_sch
SOLAR_INPUT_2
SOLAR_ADC_2
File: SOLAR_INPUT_1.kicad_sch
SOLAR_INPUT_3
SOLAR_ADC_3
File: SOLAR_INPUT_1.kicad_sch
SOLAR_INPUT_4
SOLAR_ADC_4
File: SOLAR_INPUT_1.kicad_sch
J5
USB_B_Micro
R18
330
D6
RED
Battery_charger
File: LTC4066.kicad_sch
R24
R0
BattProtect
File: BattProtect_sch.kicad_sch
Battery_NTC
BATT_TEMP
File: BATT_NTC.kicad_sch
R19
0
3.3V_Regulator
R25
0
File: LTC3130_sch.kicad_sch
CURRENTSENSOR
File: CURRENTSENSOR.kicad_sch
MPPT_5V
MPPT_PWM
File: LTC3130_sch.kicad_sch
R28
330
D7
RED
R23
0
5V_Regulator
R26
0
File: 5V_Regulator.kicad_sch
H1
MountingHole
H2
MountingHole
H3
MountingHole
H4
MountingHole
ATMEGA328
File: ATMEGA328.kicad_sch
Switches
File: Switches.kicad_sch
J7
Conn_02x10_Counter_Clockwise
Sheet: /
File: SkripsieSchematicPrototype1.kicad_sch
Title: EPS
Size: A4
Date:
Rev:
KiCad E.D.A. kicad 7.0.6
Id: 1/15

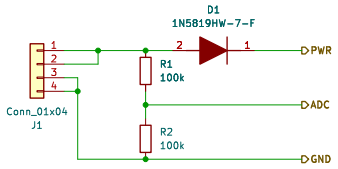

Sheet: /SOLAR_INPUT_1/
File: SOLAR_INPUT_1.kicad_sch

Title:

Size: A4	Date:	Rev:
KiCad E.D.A. kicad 7.0.6		Id: 2/15

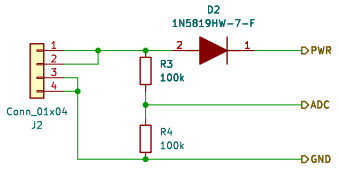

Sheet: /SOLAR_INPUT_2/
File: SOLAR_INPUT_1.kicad_sch

Title:

Size: A4	Date:	Rev:
KiCad E.D.A. kicad 7.0.6		Id: 3/15

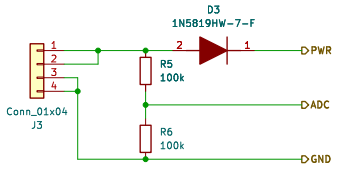

Sheet: /SOLAR_INPUT_3/
File: SOLAR_INPUT_1.kicad_sch

Title:

Size: A4	Date:	Rev:
KiCad E.D.A. kicad 7.0.6		Id: 4/15

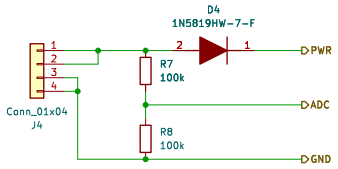

Sheet: /SOLAR_INPUT_4/
File: SOLAR_INPUT_1.kicad_sch

Title:

Size: A4	Date:	Rev:
KiCad E.D.A. kicad 7.0.6		Id: 5/15

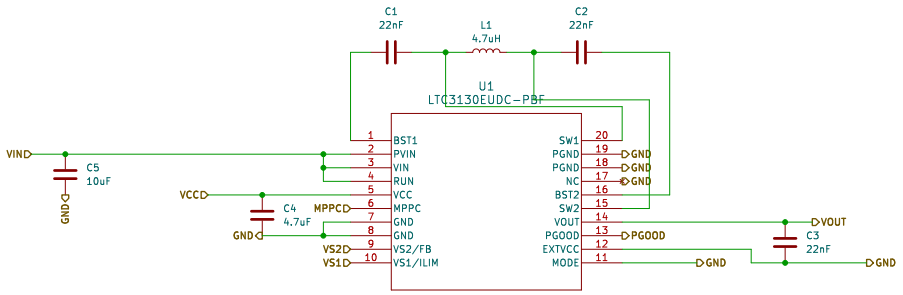

Sheet: /MPPT_5V/
File: LTC3130_sch.kicad_sch

Title: LTC3130

Size: A4	Date:	Rev:
KiCad E.D.A. kicad 7.0.6		Id: 6/15

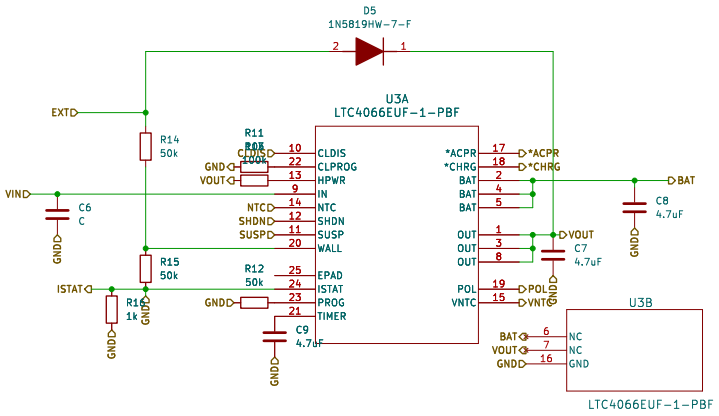

OUT (Pins 1, 3, 8): Voltage Output. This pin is used to provide controlled power to a USB device from either USB V_{BUS} (IN) or the battery (BAT) when the USB is not present. This pin can also be used as an input for battery charging when the USB is not present and a wall adapter is applied to this pin. OUT should be bypassed with at least 4.7µF to GND. Connect Pins 1, 3 and 8 with a resistance no greater than 10mΩ.

BAT (Pins 2, 4, 5): Connect to a single cell Li-Ion battery. This pin is used as an output when charging the battery, and as an input when supplying power to OUT. When the OUT pin potential drops below the BAT pin potential, an ideal diode function connects BAT to OUT and prevents V_{OUT} from dropping more than 50mV below V_{BAT}. A precision internal resistor divider sets the final float (charging) potential on this pin. The internal resistor divider is disconnected when IN and OUT are in undervoltage lockout. Connect Pins 2, 4 and 5 with a resistance no greater than 10mΩ.

POL (Pin 19): Battery Current Status Polarity Pin. This open-drain output pin indicates whether the current flowing out of the I_{STAT} pin represents one-thousandth of the current flowing into or out of the BAT pins. The POL pin will pull down when current is flowing out of the BAT pin (i.e., charging) and will assume a high impedance state when current is flowing into the BAT pin (i.e., ideal diode).

CLPROG (Pin 22): Current Limit Program and Input Current Monitor. Connecting a resistor, R_{CLPROG}, to ground programs the input to output current limit. The current limit is programmed as follows:

$$I_{CL}(A) = \frac{1000V}{R_{CLPROG}}$$

In USB applications the resistor R_{CLPROG} should be set to no less than 2.1k.

The voltage on the CLPROG pin is always proportional to the current flowing through the IN to OUT power path. This current can be calculated as follows:

$$I_{IN}(A) = \frac{V_{CLPROG}}{R_{CLPROG}} \cdot 1000$$

PROG (Pin 23): Charge Current Program. Connecting a resistor, R_{PROG}, to ground programs the battery charge current. The battery charge current is programmed as follows:

$$I_{CHG}(A) = \frac{50,000V}{R_{PROG}}$$

I_{STAT} (Pin 24): Battery Current Status Pin. One-thousandth of the current flowing into or out of the BAT pins flows out of this pin. The POL polarity pin indicates which direction current is flowing. If the current flowing into the BAT pins drops below 1mA, then the I_{STAT} pin will continue to source 1µA. The I_{STAT} pin also programs the charge current level at which the $\overline{CHRG}$ pin transitions to its high impedance state. When the I_{STAT} voltage drops below 0.1V while charging in constant voltage mode the $\overline{CHRG}$ pin will transition to a high impedance state. This corresponds to a BAT current of:

$$I_{BAT}(A) = \frac{0.1V}{R_{ISTAT}} \cdot 1000$$

Sheet: /Battery_charger/
File: LTC4066.kicad_sch

Title: LTC4066

Size: A4	Date:	Rev:
KiCad E.D.A. kicad 7.0.6		Id: 7/15

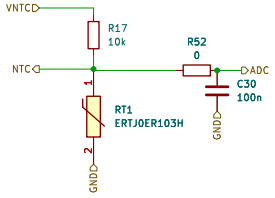

Sheet: /Battery_NTC/
File: BATT_NTC.kicad_sch

Title: NTC

Size: A4	Date:	**Rev:**
KiCad E.D.A. kicad 7.0.6		Id: 8/15

6.1 Pin Descriptions

6.1.1 Supply Input: BAT

This pin is the input supply for the device and is connected to the positive terminal of the battery pack. A 0.1-µF input capacitor is connected to ground for filtering noise.

6.1.2 Cell Negative Connection: VSS

This pin is an input to the device for cell negative ground reference. Internal circuits associated with cell voltage measurements and overcurrent protection input to differential amplifier for either Vds sensing or external sense resistor sensing will be referenced to this node.

6.1.3 Voltage Sense Node: V–

This is a sense node used for measuring several fault detection conditions, such as overcurrent charging or overcurrent discharging configured as Vds sensing for protection. This input, in conjunction with VSS, forms the differential measurement for the stated fault detection conditions. A 2.2-kΩ resistor is connected between this input pin and Pack– terminal of the system in the application.

6.1.4 Discharge FET Gate Drive Output: DOUT

This pin is an output to control the discharge FET. The output is driven from an internal circuitry connected to the BAT supply. This output transitions from high to low when a fault is detected, and requires the DSG FET to turn OFF. A 5-MΩ high impedance resistor is connected from DOUT to VSS for gate capacitance discharge when the FET is turned OFF.

6.1.5 Charge FET Gate Drive Output: COUT

This pin is an output to control the charge FET. The output is driven from an internal circuitry connected to the BAT supply. This output transitions from high to low when a fault is detected, and requires the CHG FET to turn OFF. A 5-MΩ high impedance resistor is connected from COUT to Pack– for gate capacitance discharge when FET is turned OFF.

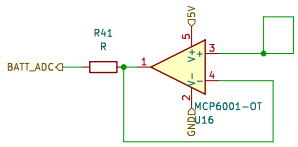

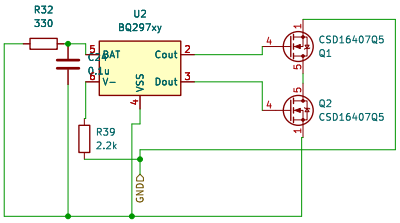

Table 10-1. Design Parameters

DESIGN PARAMETER	EXAMPLE VALUE at T_A = 25°C
Input voltage range	4.5 V to 7 V
Maximum operating discharge current	7 A
Maximum Charge Current for battery pack	4.5 A
Overvoltage Protection (OVP)	4.275 V
Overvoltage detection delay timer	1.2 s
Overvoltage Protection (OVP) release voltage	4.175 V
Undervoltage Protection (UVP)	2.8 V
Undervoltage detection delay timer	150 ms
Undervoltage Protection (UVP) release voltage	2.9 V
Charge Overcurrent detection (OCC) voltage	–70 mV
Charge Overcurrent Detection (OCC) delay timer	9 ms
Discharge Overcurrent Detection (OCD) voltage	100 mV
Discharge Overcurrent Detection (OCD) delay timer	18 ms

Table 10-1. Design Parameters (continued)

DESIGN PARAMETER	EXAMPLE VALUE at T_A = 25°C
Load Short Circuit Detection SCC) voltage, BAT to –V ≤ threshold	500 mV
Load Short Circuit Detection (SCC) delay timer	250 µs
Load Short Circuit release voltage, BAT to –V ≥ Threshold	1 V

Sheet: /BattProtect/
File: BattProtect_sch.kicad_sch

Title:

Size: A4	Date:	Rev:
KiCad E.D.A. kicad 7.0.6		Id: 9/15

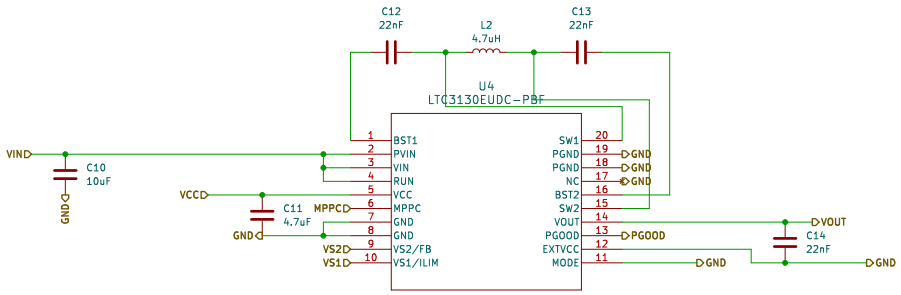

Sheet: /3.3V_Regulator/
File: LTC3130_sch.kicad_sch

Title: LTC3130

Size: A4	Date:	Rev:
KiCad E.D.A. kicad 7.0.6		Id: 10/15

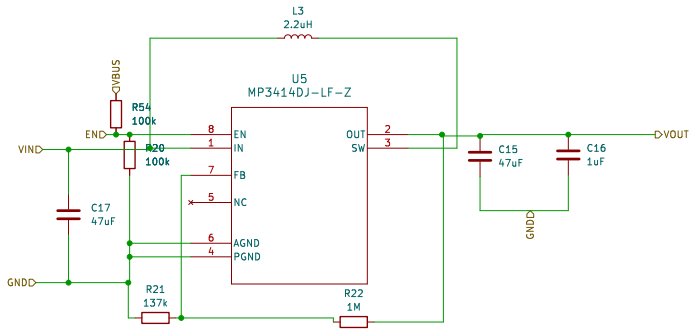

Sheet: /5V_Regulator/
File: 5V_Regulator.kicad_sch

Title:

Size: A4	Date:	Rev:
KiCad E.D.A. kicad 7.0.6		Id: 11/15

Pin Number	Description	Function
1	PC6	Reset
2	PD0	Digital Pin (RX)
3	PD1	Digital Pin (TX)
4	PD2	Digital Pin
5	PD3	Digital Pin (PWM)
6	PD4	Digital Pin
7	Vcc	Positive Voltage (Power)
8	GND	Ground
9	XTAL 1	Crystal Oscillator
10	XTAL 2	Crystal Oscillator
11	PD5	Digital Pin (PWM)
12	PD6	Digital Pin (PWM)
13	PD7	Digital Pin
14	PB0	Digital Pin
15	PB1	Digital Pin (PWM)
16	PB2	Digital Pin (PWM)
17	PB3	Digital Pin (PWM)
18	PB4	Digital Pin
19	PB5	Digital Pin
20	AVcc	Positive voltage for ADC (power)
21	AREF	Reference Voltage
22	GND	Ground
23	PC0	Analog Input
24	PC1	Analog Input
25	PC2	Analog Input
26	PC3	Analog Input
27	PC4	Analog Input
28	PC5	Analog Input

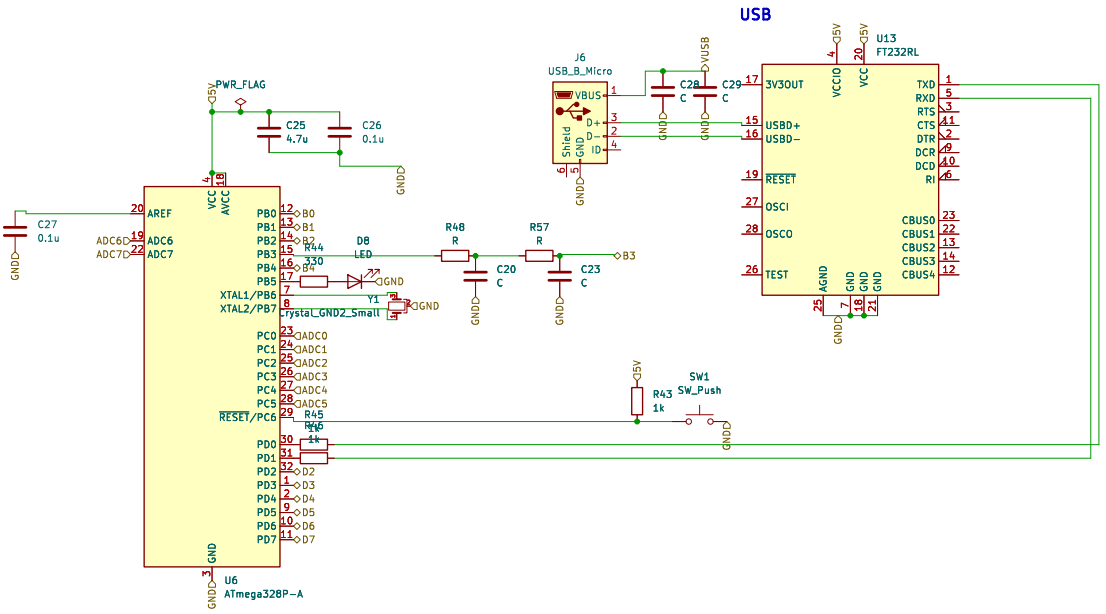

Sheet: /ATMEGA328/
File: ATMEGA328.kicad_sch

Title: ATMEGA328

Size: A4	Date:	Rev:
KiCad E.D.A. kicad 7.0.6		Id: 12/15

The absolute maximum current is 4 A per distribution line, as determined by the connector specification assuming a maximum internal temperature of 60 °C [6]. The allowed current levels can however be lower due to the battery limitations and the power budget. It is recommended to include programmable current limiters for each distribution line.
In-rush current limits are not yet specified in this standard. Therefore, the specifications of the chosen central electrical power distribution unit needs to be followed. It is generally recommended to limit the in-rush current as much as possible at the subsystem loads.

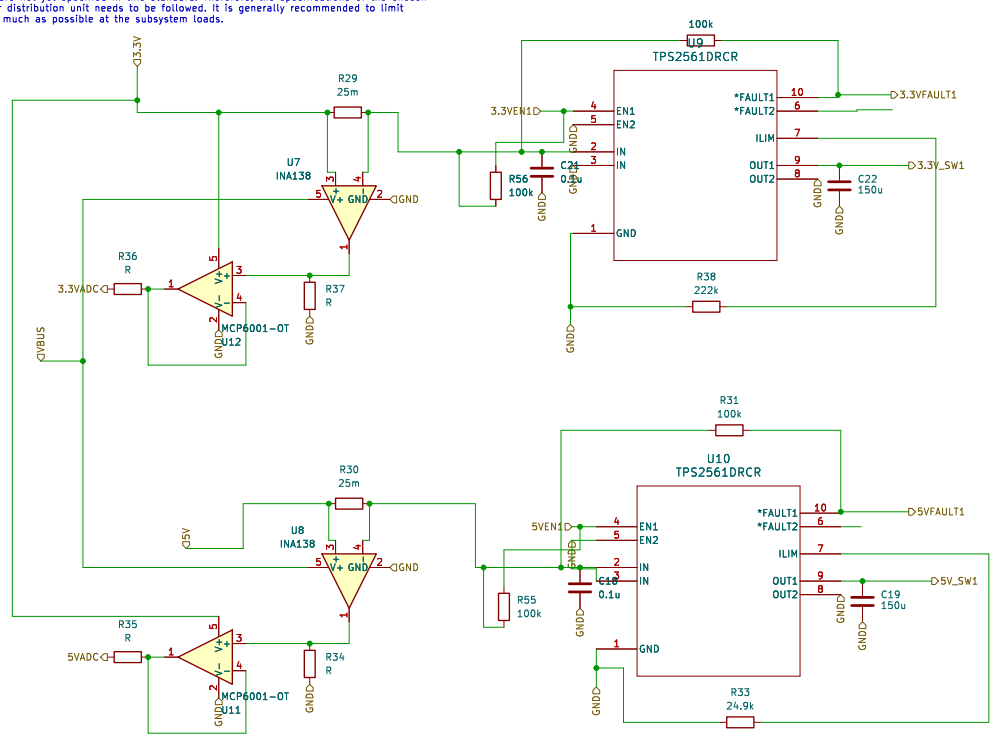

$$I_{OSmax}(mA) = \frac{52850V}{R_{ILIM}^{0.957} k\Omega}$$

300mA current limit

Table 10-1. Design Parameters

PARAMETER	VALUE
Input voltage	5 V
Output voltage	5 V
Above a minimum current limit	2000 mA
Below a minimum current limit	1000 mA

SWITCH OF MANUALLY (Microcontroller EN + ADC) OR AUTOMATIC (TPS switch programmed)

Sheet: /Switches/
File: Switches.kicad_sch

Title: Switches

Size: A4 | Date: | **Rev:**
KiCad E.D.A. kicad 7.0.6 | Id: 13/15

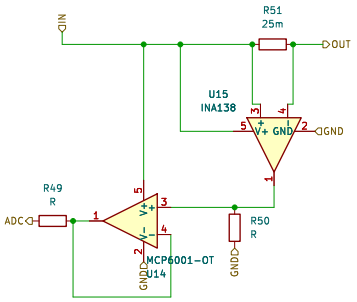

Sheet: /CURRENTSENSOR/
File: CURRENTSENSOR.kicad_sch

Title:

Size: A4	Date:	Rev:
KiCad E.D.A. kicad 7.0.6		Id: 14/15

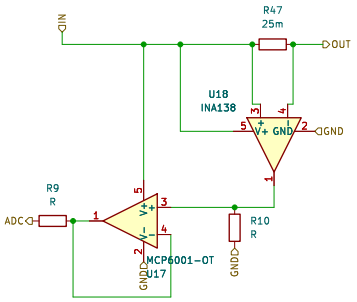

Sheet: /CURRENTSENSOR1/
File: CURRENTSENSOR.kicad_sch

Title:

Size: A4	Date:	Rev:
KiCad E.D.A. kicad 7.0.6		Id: 15/15

Appendix F

Code

```
#include <Arduino.h>

// Define pins for PWM output, current sensor, and voltage sensor
const int pwmPin = 9;
const int currentSensorPin = A0;
const int voltageSensorPin = A1;

// Variables for storing previous measurements
float prevCurrent = 0.0;
float prevVoltage = 0.0;
float prevPower = 0.0;

// Set initial PWM duty cycle
int pwmDutyCycle = 128; // Adjust as needed

void setup() {
  // Initialize PWM pin
  pinMode(pwmPin, OUTPUT);

  // Initialize Serial communication for debugging
  Serial.begin(9600);
}

void loop() {
  // Read current and voltage
  float current = analogRead(currentSensorPin) * (5.0 / 1023.0);
  float voltage = analogRead(voltageSensorPin) * (5.0 / 1023.0);

  // Calculate power
  float power = current * voltage;
```

```
  // Compare power with previous measurements
  if (power > prevPower) {
    // Increase PWM duty cycle for higher power
    pwmDutyCycle += 5; // Adjust the increment as needed
  } else if (power < prevPower) {
    // Decrease PWM duty cycle for lower power
    pwmDutyCycle -= 5; // Adjust the decrement as needed
  }

  // Update PWM output
  analogWrite(pwmPin, pwmDutyCycle);

  // Store previous measurements
  prevCurrent = current;
  prevVoltage = voltage;
  prevPower = power;

  // Print measurements for debugging
  Serial.print("Current: "); Serial.print(current); Serial.print(" A\t");
  Serial.print("Voltage: "); Serial.print(voltage); Serial.print(" V\t");
  Serial.print("Power: "); Serial.print(power); Serial.print(" W\t");
  Serial.print("PWM Duty Cycle: "); Serial.println(pwmDutyCycle);

  // Add a delay to control the loop execution frequency
  delay(1000); // Adjust as needed
}
```

Click 3.2.2 to return to MPPT software.